THE IMPACT OF BUFFER ZONE CHANGES ON THE ARCHITECTURE OF THE PALEOZIC LOWER CUTLER BEDS OF UTAH

by

SIAVASH RASTAGHI

Presented to the Faculty of the Graduate School of

The University of Texas at Arlington in Partial Fulfillment

of the Requirements

for the Degree of

MASTER OF SCIENCE IN GEOLOGY

THE UNIVERSITY OF TEXAS AT ARLINGTON

December 2011

ACKNOWLEDGEMENTS

I am highly indebted to Dr. John M. Holbrook, my thesis advisor and committee chairman, for his unlimited support, encouragement, advice and guidance without whom this research was not possible. I would also like to express my gratitude to Dr. Nigel Mountney and the University of Leeds for providing me with the area of study, along with Oliver Wakefield for field guidance. I am grateful to my committee members Dr. John Wickham and Dr. Merlynd Nestell for being part of this research and contributing to the quality of this research paper. I would also like to give my appreciation to Dr. Larry Standlee and Helen Hough for their support and assistance.

Finally, I dedicate this research to my parents Abdolah and Roohbakhsh, my brothers Darioush and Kourosh without whose constant support I could not have achieved this thesis.

November 2011

ABSTRACT

THE IMPACT OF BUFFER ZONE CHANGES ON THE ARCHITECTURE OF THE PALEOZIC LOWER CUTLER BEDS OF UTAH

Siavash Rastaghi, M.S.

The University of Texas at Arlington, 2011

Supervising Professor: John M. Holbrook

The Shafer basin fluvial units, as being part of the Paradox fold and fault belt basin, received sediments from alluvial fans through mixed braided-meandering river systems that eroded the clastic rocks of the Uncompahgre highlands to the northeast and flowed southwestward through aeolian dune fields to an open sea during Pennsylvanian to early Permian time. The best exposed rocks of the Lower Cutler beds were photographed and investigated along the Colorado River in the Shafer and Canyonland basins. The Architectural Element Analysis technique was used to categorize bounding surface orders, and to identify lithofacies and fluvial elements such as lateral accretion bars, channels and overbank deposits. Both merged photographs and outcrop panel drawings were used for this project. The objective of the method was to dissect fluvial sand-sheets and to characterize their origin and the depositional environment under which they were deposited. Therefore, Architectural Element Analysis was applied to the FL2 interval of the Permian Cutler Group in two Shafer basin locations (Potash and Goose Neck) and to the FL3 interval in the Canyonland basin location of Utah. In the Goose Neck fluvial unit, a ~thirty five meters long and ~five meter deep valley incision surface bisects the section into two intervals of mixed meandering and braided bars. Moreover, numerous mid-channel bars on the top of the FL2 strata are indirect evidence of a

transition toward braided systems at the top. Similarly, the ~seven meters thick Potash section is bisected by multiple nested-valley surfaces bound by a regional sequence boundary. The multiple valleys are filled by several channel belt (CB), and channel fill elements such as downstream accretion bar element (DA), overbank, etc. that are produced by progressive transitions between braided and meandering paleo-rivers.

The base of all of the fluvial units is punctuated by a regional sequence boundary. The fluvial sequence boundary was created through paleo-river re-washing and removing of dry aeolian and deeper buried interdune sand-sheets in places. The sequence boundary records a hiatus at the base of the FL2 interval; however, it is not punctuated by erosion, but rather by a facies transition and aggradation of the Canyonland rocks, the FL3 strata landward. This discrepancy may be explained by the strata's location relative to the paleo-sea level shoreline, subsiding basin, and sediment source. The change in the rivers profile related to cycles in sediment/discharge ratio caused incision and aggradation at a higher frequency than the rate of subsidence. This process resulted in cut and fill of buffer valleys concurrent with an overall trend of aggradation tied to continued subsidence. The result is aggradation punctuated by periods of incision during sand-sheet deposition. This result contrasts with traditional models of fluvial aggradation and deposition of low-accommodation sandstone sheets that presume these sheets are accumulated by linear progressive stacking. The Lower Cutler deposits in the Shafer basin thus represent aggradation by stacking of channel deposits and their incision by high order valley surfaces that shows regional changes in paleo-river dynamics. Permian fluvial strata are marked by higher-order surfaces of re-incision in what otherwise appear to be progressively stacked channel belts.

The last phase of FL3 deposition is marked by severe seismic activity. The liquefaction of bars at the top of the interval confirms that the basin was active at the time of FL3 deposition and that a high frequency earthquake greater than 6.5Mo likely occurred.

TABLE OF CONTENTS

LIST OF ILLUSTRATIONS

Figure Page

LIST OF TABLES

Table Page

CHAPTER 1

INTRODUCTION

Virgilian-Wolfcampian fluvial rocks of the Lower Cutler beds are interpreted to have been deposited by rivers that transported sediments in alluvial fans extending from the Uncompahgre uplift in a southwestern paleo-direction (Mack, 1977) (Figure 1) This research investigates the Lower Cutler beds in three locations (Figure 2). Two fluvial outcrops are in the Shafer basin (Figure 3), and one in the Canyonland (Figure 4). The inquiry empowered by Architecture Element Analysis will clarify the paleo-river systems that have created mixed braided/meandering bars in the subsiding Shafer and Canyonland basins. It will also illustrate their magnitude and their spatial variance within the buffer zone that dictates the FL2 and FL3 fluvial architecture. In another words, FL2 and FL3 will be compared and contrasted in terms of downstream sea-level buttress controls versus climate.

Of special interest in the study of the Lower Cutler beds fluvial formations was the second stratigraphic unit FL2 of the Shafer basin (Jordan and Mountney, 2010) (Figure 7 and 8) and the uppermost fluvial unit, FL3, in Canyonland National Monument, respectively (Figure 4). Rocks of the Lower Cutler beds were photographed and investigated along the Colorado River in the Shafer and Canyonland basins. Both fluvial locations in the Shafer basin (Potash, and Goose Neck) are expressed as elongated sheets throughout the area. Marine transgressive facies also separate both aeolian and fluvial strata in the Lower Cutler beds (Jordan and Mountney, 2010). The heterolithic strata generated by these transgressive, regressive fluvial and aeolian units within the Lower Cutler beds have complex architecture (Jordan and Mountney, 2010). Although there is an abundance of literature about the Lower Cutler beds aeolian sand dunes and their origins, the fluvial units have not been extensively researched in terms of their fundamental architecture, fluvial patterns, and spatial variation within buffer zones.

Thus, the investigation was undertaken to gain a better understanding of the complex Lower Cutler fluvial deposits and to redefine the nature of the paleo-rivers that flowed and filled the Shafer and Canyonland basins. Specifically, this is an investigation to organize the fluvial styles (channel fill, channel, channel belt, valley etc.), to create a 3-D fluvial bar model, and to identify the prime controlling mechanism of their deposition. The application of Architectural Element Analysis (AEA) and lithofacies associations will also cast light on the Lower Cutler beds strata and will aid in constructing models based on modern sedimentary environments that are used as analogs for characterization of ancient fluvial rocks.

1.1 Background and previous works

The Lower Cutler beds are exposed in southeastern Utah within the Paradox basin, the northern part of which is termed the Paradox fold and fault belt (Kelley, 1958a) (Figure 1). The Paradox basin in the Early Permian was situated just north of the equator and was rotated as much as 45° clockwise from its present orientation (Condon, 1997). The Lower Cutler beds were originally named the Rico Formation (McKnight, 1958).

The Shafer basin fluvial units, as being part of the Paradox basin, were bounded on the northeast by the Uncompahgre uplift of the ancestral Rocky Mountains during Pennsylvanian to Early Permian time (Barbeau, 2003) (Figure 1). Alluvial fans fed the basin with sediment through a braided river system (Mack, 1977) that eroded the clastic rocks of the Uncompahgre highlands to the northeast and flowed southwestward through aeolian dune fields to an open sea (Terrell, 1972) (Figure 5).

FL2 fluvial strata are in the Potash location in the Shafer basin. The studied strata are about 19 km to the city of Moab in the southeast part of Utah. The FL2 unit in the Shafer basin (Goose Neck) is approximately 21 km to the southwest of Moab along the Colorado River. Finally, the Canyonland fluvial unit is situated just about 41 km southwest of Moab in the Canyonland basin (Figure 2 and 4).

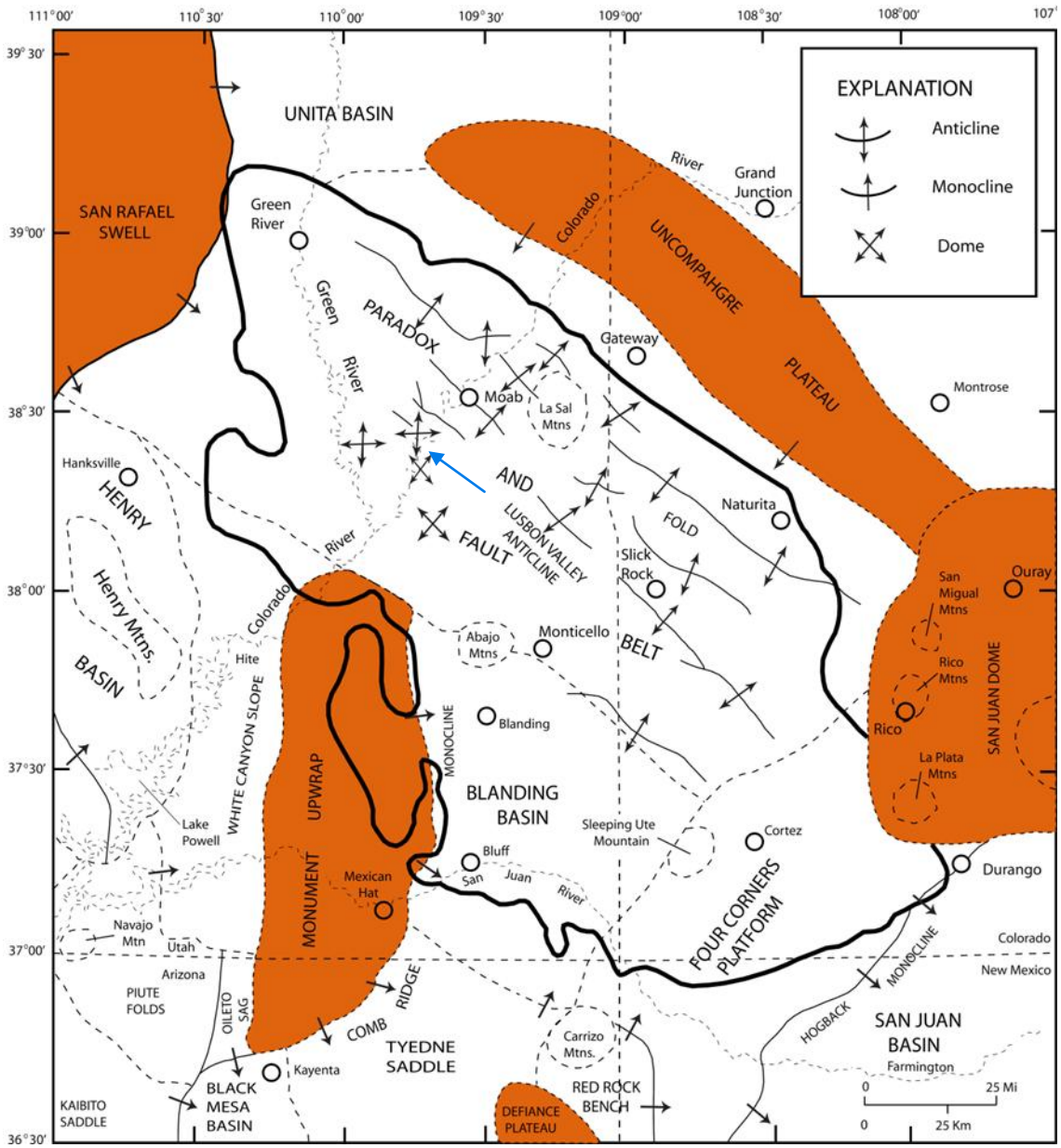

Figure 1: Paradox basin structural map shows Lower Cutler beds sediment source in the Uncompahgre uplift to the northeast juxtaposed to the basin which filled the Paradox basin through alluvium. Blue arrow shows the studied area in the Shafer basin (modified from Kelly, 1958).

Aeolian dunes commonly occupied dune fields in the distal portions of the basin comprising south-easterly migrating trends (Loope, 1984, 1985). These dune fields were

flanked on their western margin by a shallow sea that periodically transgressed eastward across low-relief parts of the basin plain (Loope, 1984) (Figure 5).

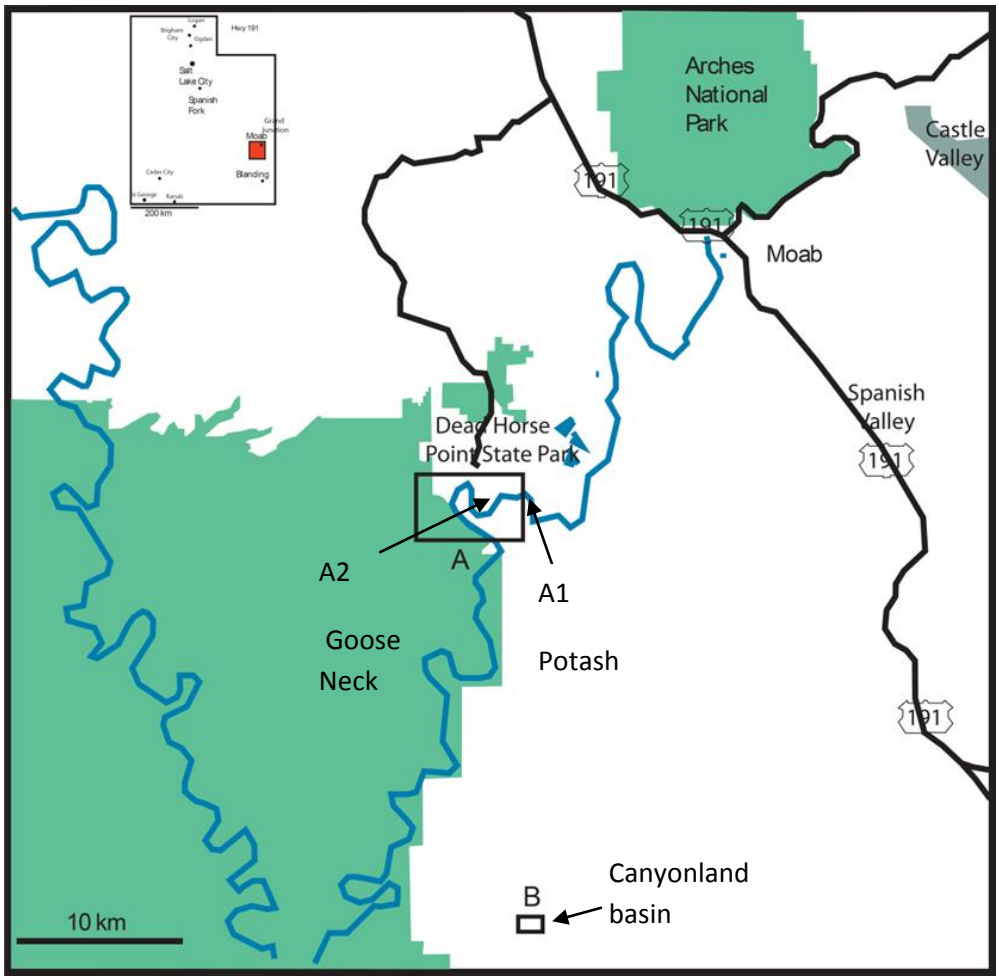

Figure 2: Two boxes on the map represent the studied area. Upper box contains A1 and A2 locations (Potash and Goose Neck) and location B in the Canyonland basin.

Deflation surfaces recording dune erosion to the surface of water table (Loope, 1985) are abundant and are indirect results of sea-level changes (Langford and Chan, 1989). The initial sea-level drop caused a drop in the water table and more down-cutting of the fluvial systems and erg progradation because of mobilization of sand. With sea-level rise, sand was

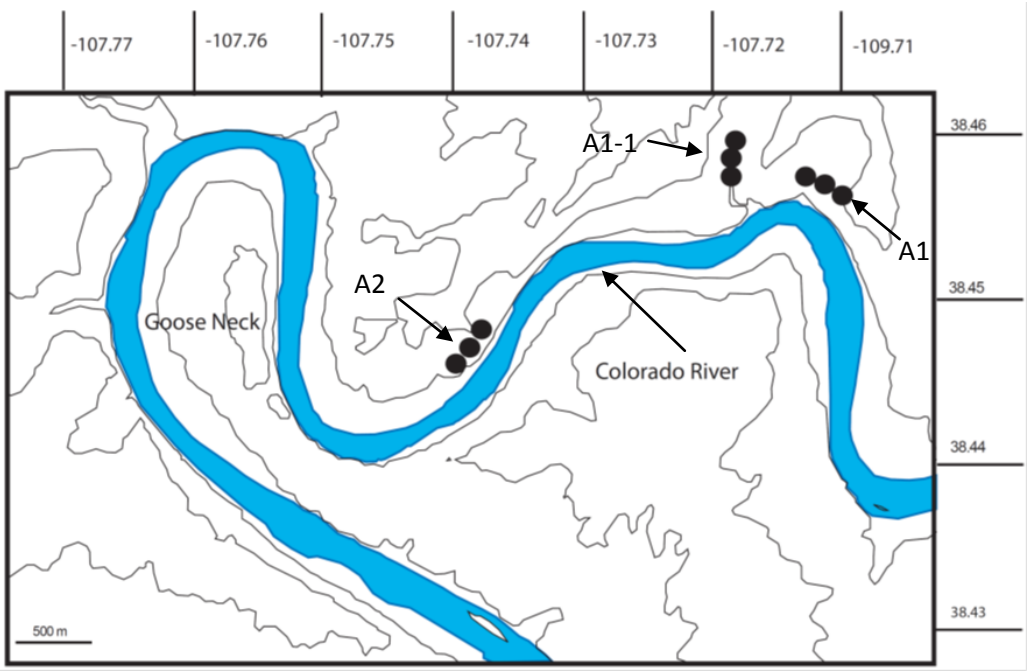

Figure 3: (A1 - A1-1) are studied Lower Cutler beds in the Shafer basin (Potash) and (A2) is the same fluvial unit in the Shafer basin (Goose Neck) location.

saturated and sand drift as a source to feed aeolian ergs halted. In addition, depletion of the sediment supply produced a deflation surface that was colonized by vegetation. Transgression also shifted facies basin-ward, and that movement produced sand-starved conditions and downwind–progressing deflation surfaces (Langford and Chan, 1989) (Figure 6).

1.2 Lithofacies

The Lower Cutler beds end with the Cedar Mesa limestone, which is overlain by the beds of Upper Cutler Group strata called the Cedar Mesa Sandstone. The Cedar Mesa Sandstone, Organ Rock Formation and White Rim Sandstone are in the Upper Cutler Group and are not investigated in this project. Lithofacies of the Lower Cutler beds are strata above the Hermosa bed, or equivalent aged rocks, and are a mix of quartzose and arkosic sandstone and minor conglomerate, mudstone, siltstone, and limestone (Mack, 1978; Cain and Mountney, 2009). The Lower Cutler beds are the medial to distal deposits of the Cutler Formation (undivided) and are the lowermost part of the Upper Cutler Group (Figure 9).

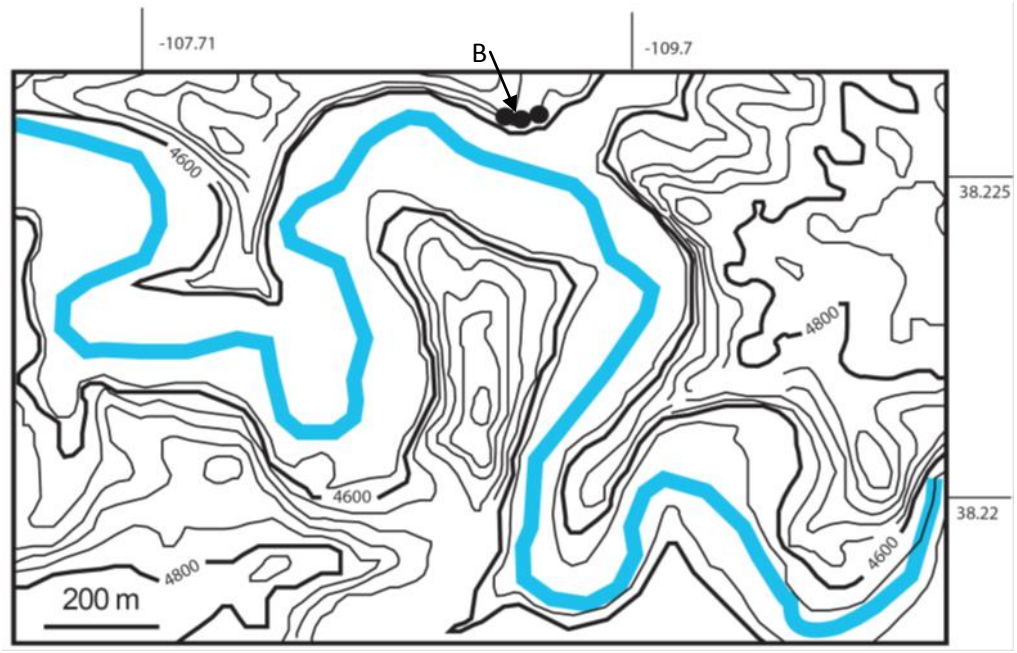

Figure 4: Topographic map showing the location of the studied Lower Cutler beds in the Canyonland basin.

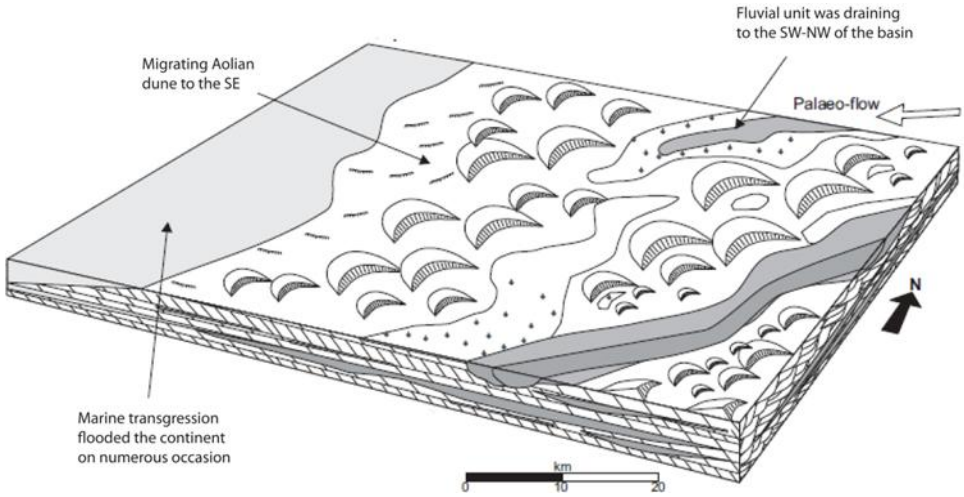

Figure 5: General paleo-direction of barchan dunes and fluvial river at the time of Lower Cutler beds deposition (Jordan and Mountney, 2010).

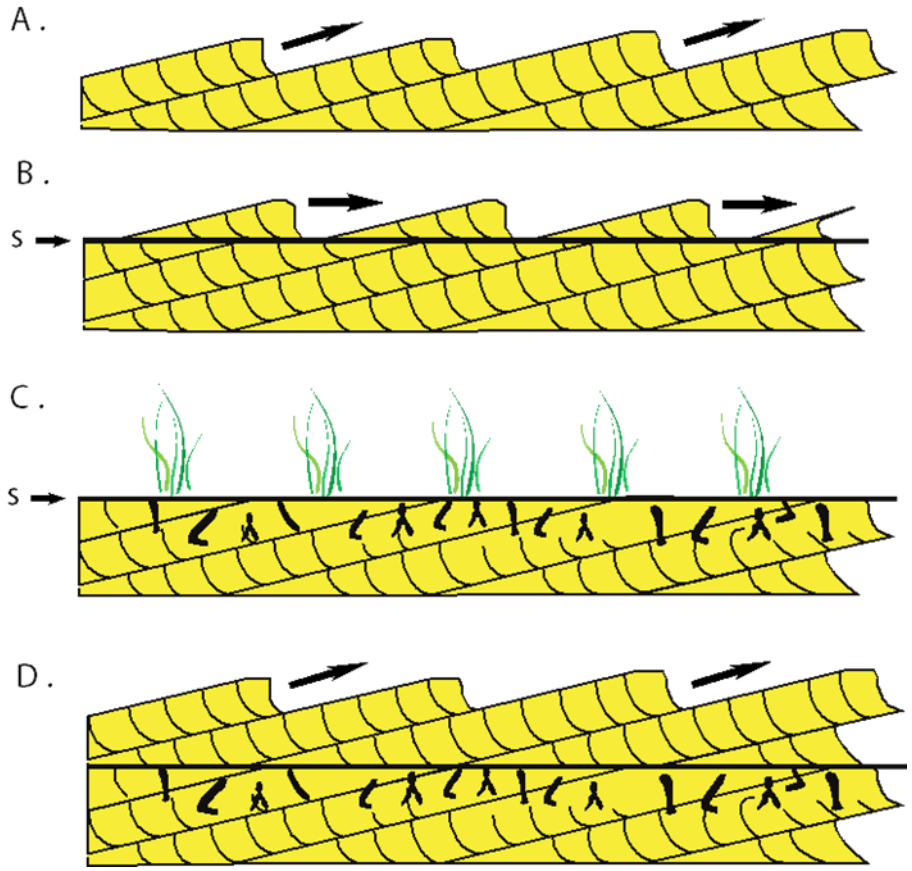

Figure 6: Model illustrating the formation of deflationary super surfaces in aeolian sandstone, modified from Langford and Chan (1989). Dunes cease to climb and interdunes climb while migrating and they preserve underlying dune deposits. (A) First order surfaces separate dune foresets, (B) Continued migration of dunes without deposition truncates first order surfaces, (C) Non deposition or erosion occurs. Deflation to ground water table results in a low relief erosion surface, (D) Growth of vegetation on deflation surface creates bioturbated horizons beneath the erosion surface.

1.3 Stratigraphy

There are ten reported shallow marine transgressions in the Paradox basin (Jordan and Mountney, 2010). There are three common facies transitions in the basin: (I) marine-fluvial, (II) marine-aeolian, and (III) aeolian-fluvial (Jordan and Mountney, 2010). Loope (1984) has found five major facies associations. However, Cain and Mountney (2009) recognized eight lithofacies in the Lower Cutler beds of the Paradox basin and three lithofacies associations, fluvial, aeolian, and marine, which is consistent with this study (Figure 16 and17).

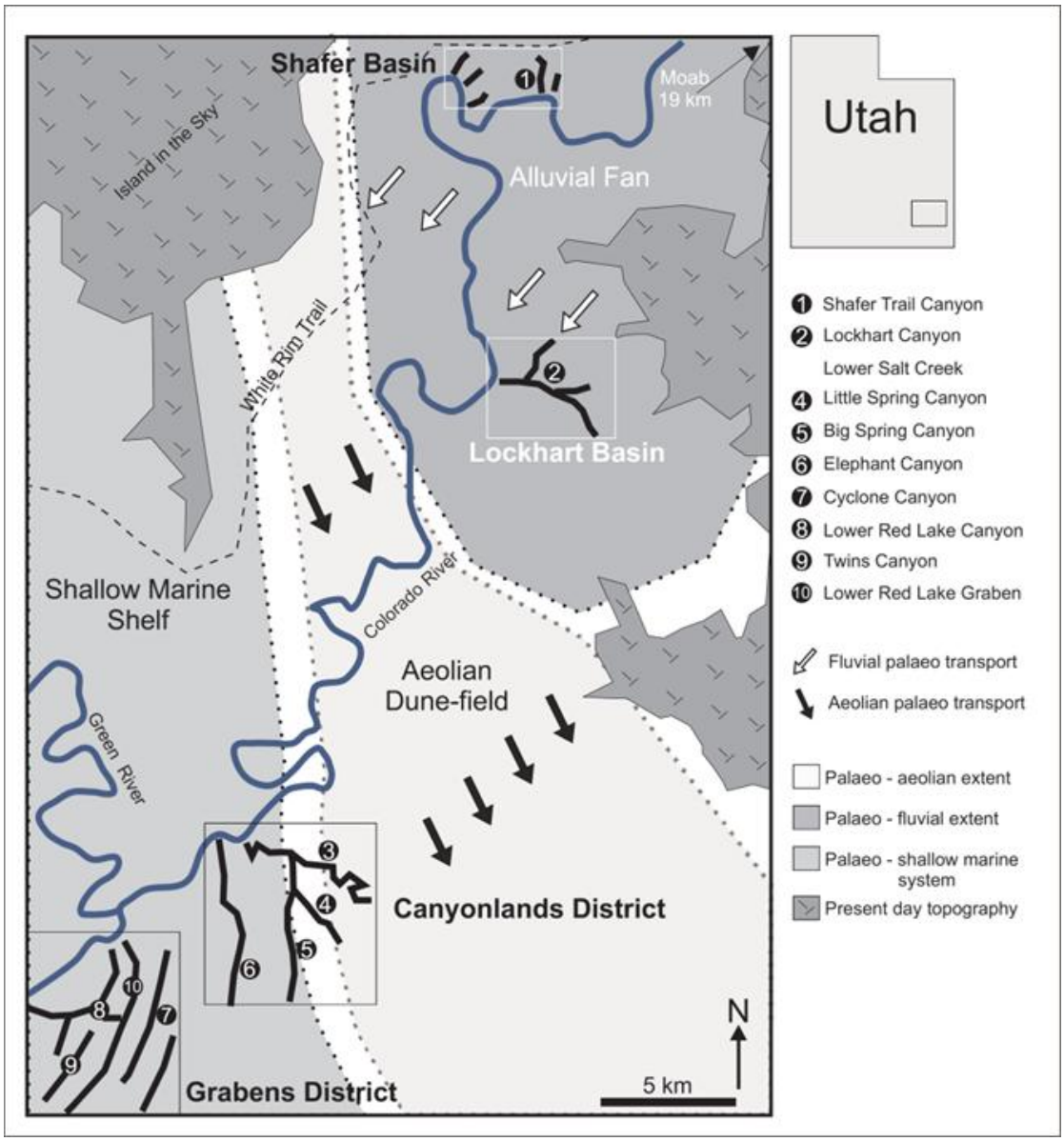

Figure 7: Investigated dominant sedimentology within the Paradox basin along the modern Colorado River (Jordan and Mountney, 2010).

The fluvial association is comprised of multiple valley, channel belt, channel surfaces and channel fill elements with overlying and underlying aeolian association. Aeolian facies are large trough and planar cross-bedded dunes, and sand-sheet facies that are interpreted to be interdune deposits (Hunter, 1977; Jordan and Mountney, 2010). The transgressive marine association includes deposits of carbonate ramp, channel mouth bar, and shallow marine fine-

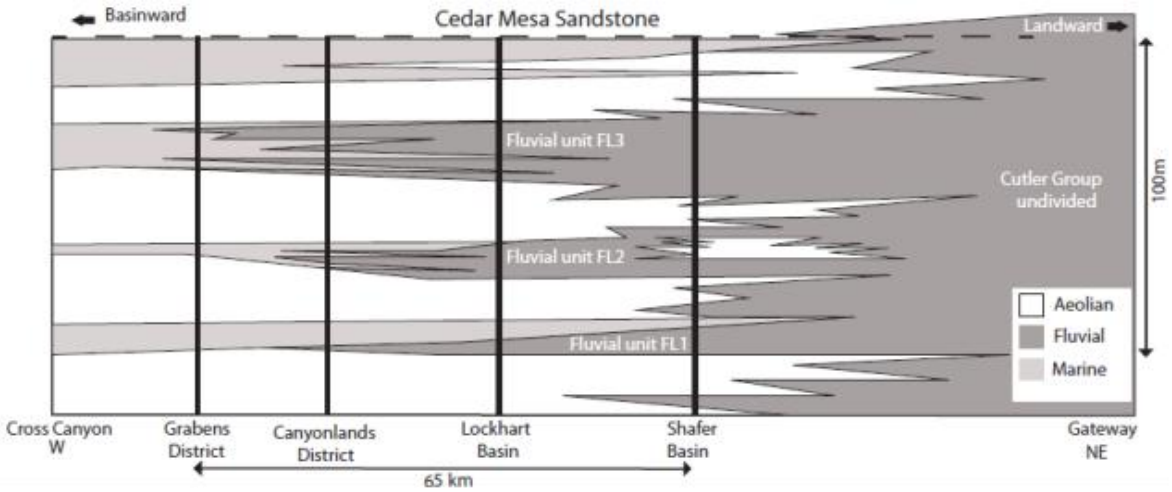

Figure 8: Schematic cross-section of the Lower Cutler beds. The studied fluvial strata may actually be a section of undifferentiated fluvial unit FL2 and FL3 proposed by Jordan and Mountney (2010).

grained mudstone (Terrell, 1972; Mack, 1977; Loope, 1984; Halley and Schmoker, 1983; Tucker et al., 1990; Bromley, 1996; Clarkson et al., 1998).

Generally, the genetic units of the Cedar Mesa, Lower Cutler beds and Upper Honaker Trail Formation (Hermosa) had vertical accretion rates of several centimeters per year and could have been deposited during periods of heavy sand influx that were triggered by the regression of sea level simultaneously with an ongoing subsiding basin (Loope, 1985). If marine/non-marine cycles in the Rico and Hermosa bed are analogous to cycles of similar ages in neighboring regions, their transgressive/regressive cycles were in the range of 400,000 to 800,000 years (Loope, 1985). The T/R cycles then can be of the 4th and the Lower Cutler beds strata were produced by tectonic and eustatic processes of 3rd-order Milankovitch cycle (Table 1).

Mineral measurements indicate that there is as much as a 50% decrease in the percentage of high density minerals between the non-marine Cutler Formation (Permian) and its lithofacies equivalent, the marine Cedar Mesa Sandstone, in the vicinity of Moab, Utah (Mack, 1978) (Figure 10). The significant change in mineralogy from heavy fragments near the sediment source to the feldspar deposited away maybe the byproduct of an active reworking of

sediments in a shallow marine environment. The increase of compositional maturation to the south and southwest part of the Permian Cutler beds in Moab was produced by mechanical breakage and recycling of the grains (Mack, 1977).

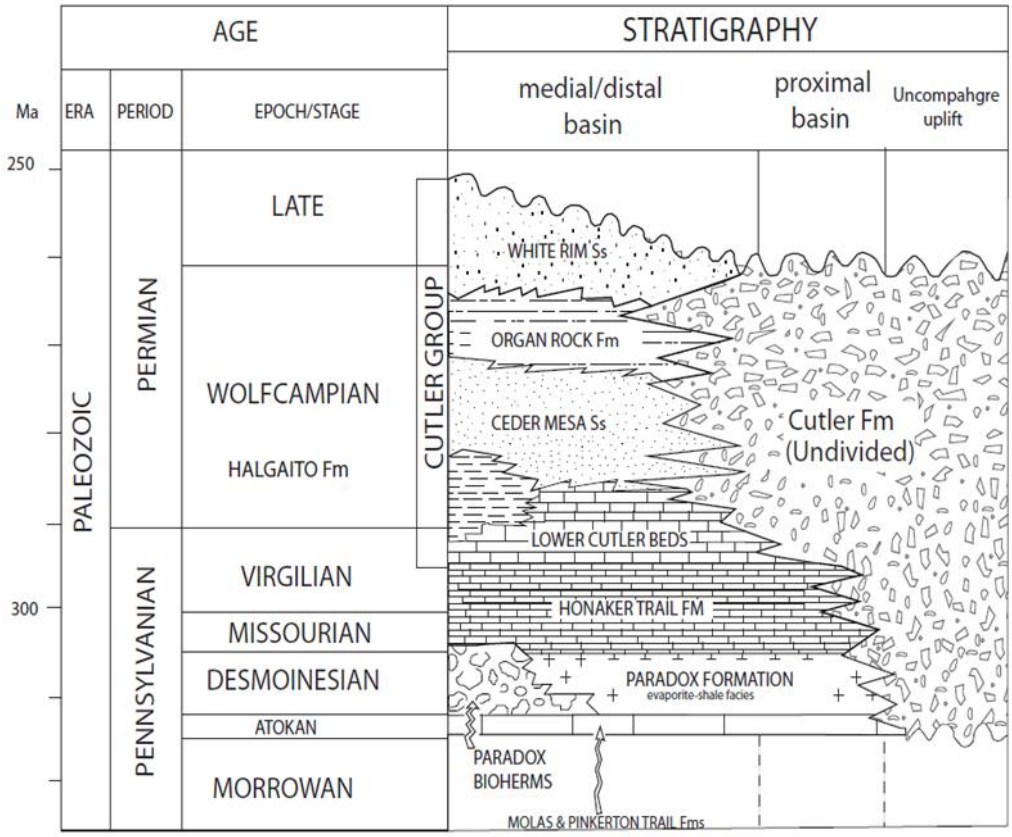

Figure 9: Stratigraphic column of basin-fill units in the Paradox basin. Compiled from Wengerd and Matheny (1958), Pray and Wray (1963), Elias (1963), Peterson and Hite (1969), and Condon (1997).

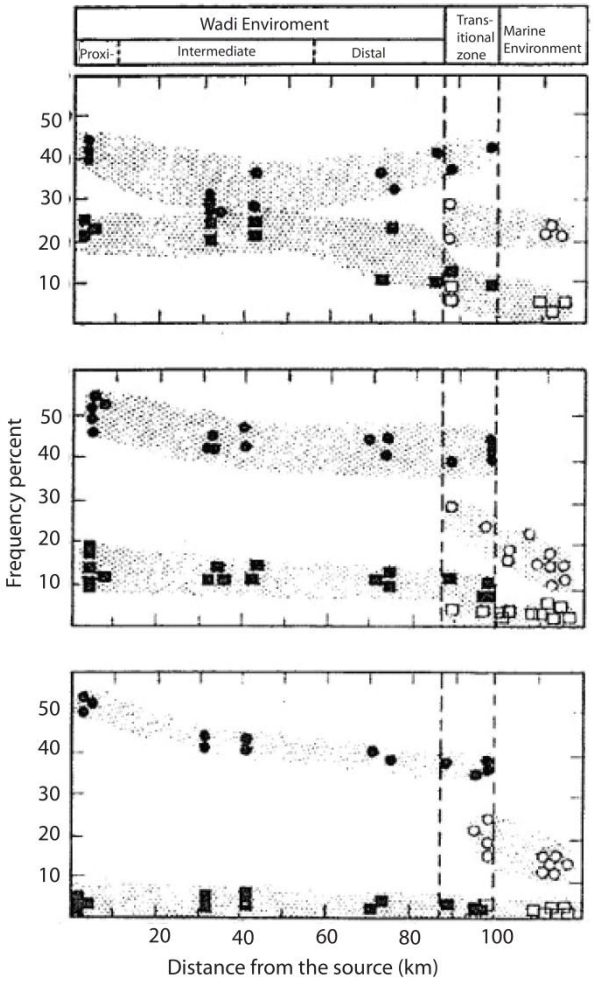

Figure 10: Change in relative percentage of total feldspar (circles) and total rock fragments (squares) as a function of distance from the source in the braided system and shallow marine environment. Upper diagram: Coarse sand size fraction; middle diagram: Sand-size fraction; lower diagram: Fine sand-size fraction (Mack, 1978).

CHAPTER 2

METHODS

Architectural Element Analysis is a technique that was used in this research to interpret the deposition of fluvial strata. An architectural element is defined as a depositional system equal to channel fill components like thalwegs, depositional bars, overbank , and typically larger than one lithofacies unit, trough cross-bedded sandstone (St), ripple marks (Sr), etc. (Miall, 1985). Furthermore, Architectural Element Analysis is a method that investigates facies assemblage, internal geometry, and external form within third- through fifth-order bounding surfaces containing other smaller-order surfaces and sedimentary structures within a fluvial/deltaic depositional unit (Figure 12, Table 1). The lower and upper bounding surfaces maybe concave up, convex up, erosional, planar and irregular (Miall, 1985, 1988a, 1988b, 1991b) (Figure 11, 12, 13, Table 1).

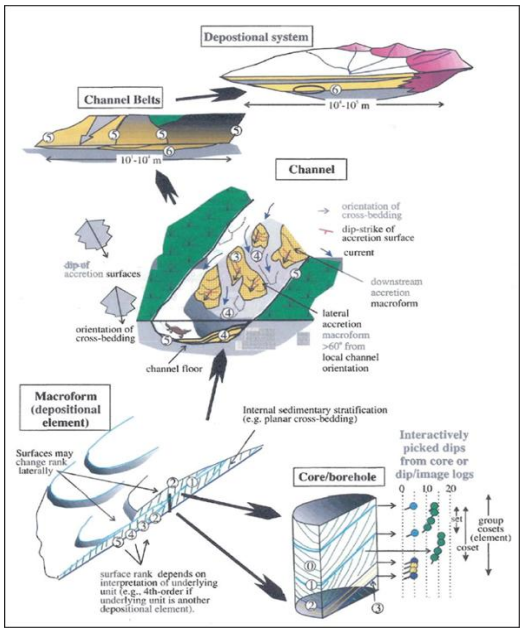

Figure 11: Hierarchy and dissection of a large scale depositional system to small bed forms defined by Architectural Element Analysis (Miall, 1985).

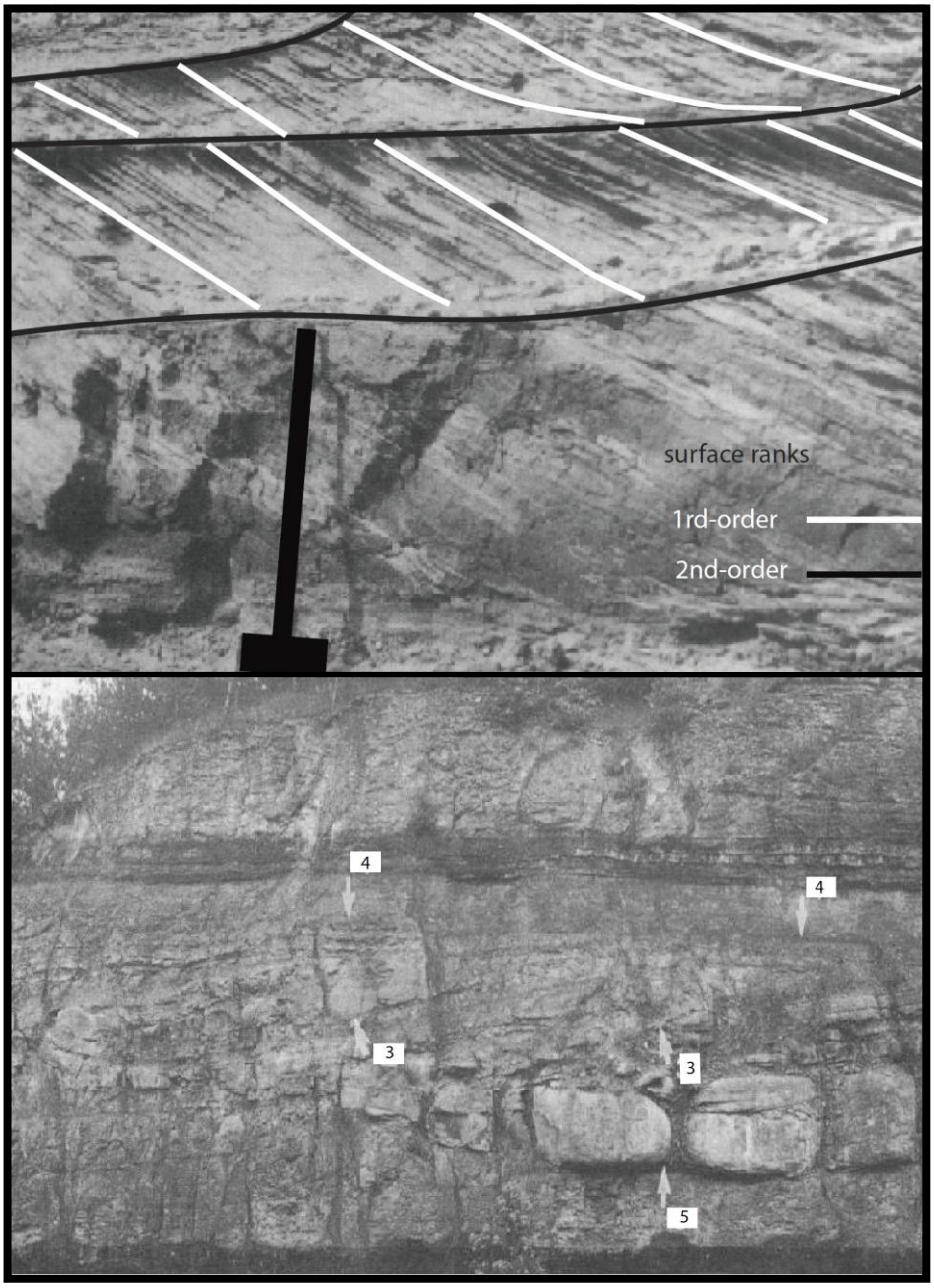

Figure 12: From the top: First-order surface within a microform that creates cross- bed set bounding surfaces that represent trains of sedimentary bedforms. 2nd-order is a surface that truncates first-order surface, or first-order surface lap down on it. 2nd-order bounding surface is associated with minor change in flow direction (Table 2). Lower photo: 3rd through 5th-order bounding surfaces. 3rd-order is a surface that binds first-to-second order bounding surface. 3rd-order normally down-lap on the cut-bank channel (5th -order) and is associated with erosional macroform surfaces (Miall, 1985, 1988a, 1988b). Refer to Figure 14 and Table 2

Table 1: Hierarchy of depositional units based on time scale of processes, sedimentation rate and rank of each bounding surface in alluvial deposits (Miall,1991).

Hierarchy of a depositional unit in alluvial deposits (modified from Miall, 1991)					
Grp	Time scale of process (a)	Examples of processes	Instan-taneous sedimentation rate (m/ka)	Fluvial, deltaic depositional units	Rank and characteristics of bounding surfaces
1	10^{-6}	Burst sweep cycle			0th-order, lamination surface
2	10^{-5} – 10^{-4}	Bedform migration	10^{5}	Ripple (microform)	1st-order, set bounding surface
3	10^{-3}	Bedform migration	10^{5}	Diurnal dune increment, reactivation surface	1st-order, set bounding surface
4	10^{-2} – 10^{-1}	Bedform migration	10^{4}	Dune (mesoform)	2nd-order, coset bounding surface
5	10^{0} – 10^{1}	Seasonal events, 10-year flood	10^{2-3}	Macroform growth increment	3rd-order, dipping 5-20° in direction of accretion
6	10^{2} – 10^{3}	100-year flood, channel and bar migration	10^{2-3}	Macroform, e.g.,point bar, Levee, splay immature paleosol	4th-order,convex-up macroform top, minor channle scour,flat surface bounding floor plain elements
7	10^{3} – 10^{4}	Long-term geomorphic processes,e.g. channel avulsion	$10^{0} – 10^{1}$	Channel, delta lobe, mature paleosol	5th-order, flat to concave up channel base
8	10^{4} – 10^{5}	5th-order (Milankovitch) cycle,response to fault pulse	10^{-1}	Channel belt, alluvial fan, minor sequence	6th-order, flat,regionally extensive, or base of incised valley
9	10^{5} – 10^{6}	4th-order (Milankovitch) cycle,response to fault pulse	$10^{-1} – 10^{-2}$	Major dep system, fan tract, sequence	7th-order, sequence boundary, flat,regionally extensive, or base of incised valley
10	10^{6} – 10^{7}	3rd-order cycles. Tectonic and eustatic processes	$10^{-3} – 10^{-2}$	Basin-fill complex	8th-order, regional disconformity

The history of architectural elements and bounding surfaces starts with Brookfield (1977) who was the first to apply bounding surfaces and their hierarchical orders to aeolian dune sets. Allen (1983) was the first author to use the term fluvial architecture as geometry and internal strata of channel and over-bank deposits that could be arranged into genetically related strata from others by bedding contact (Figure 14).

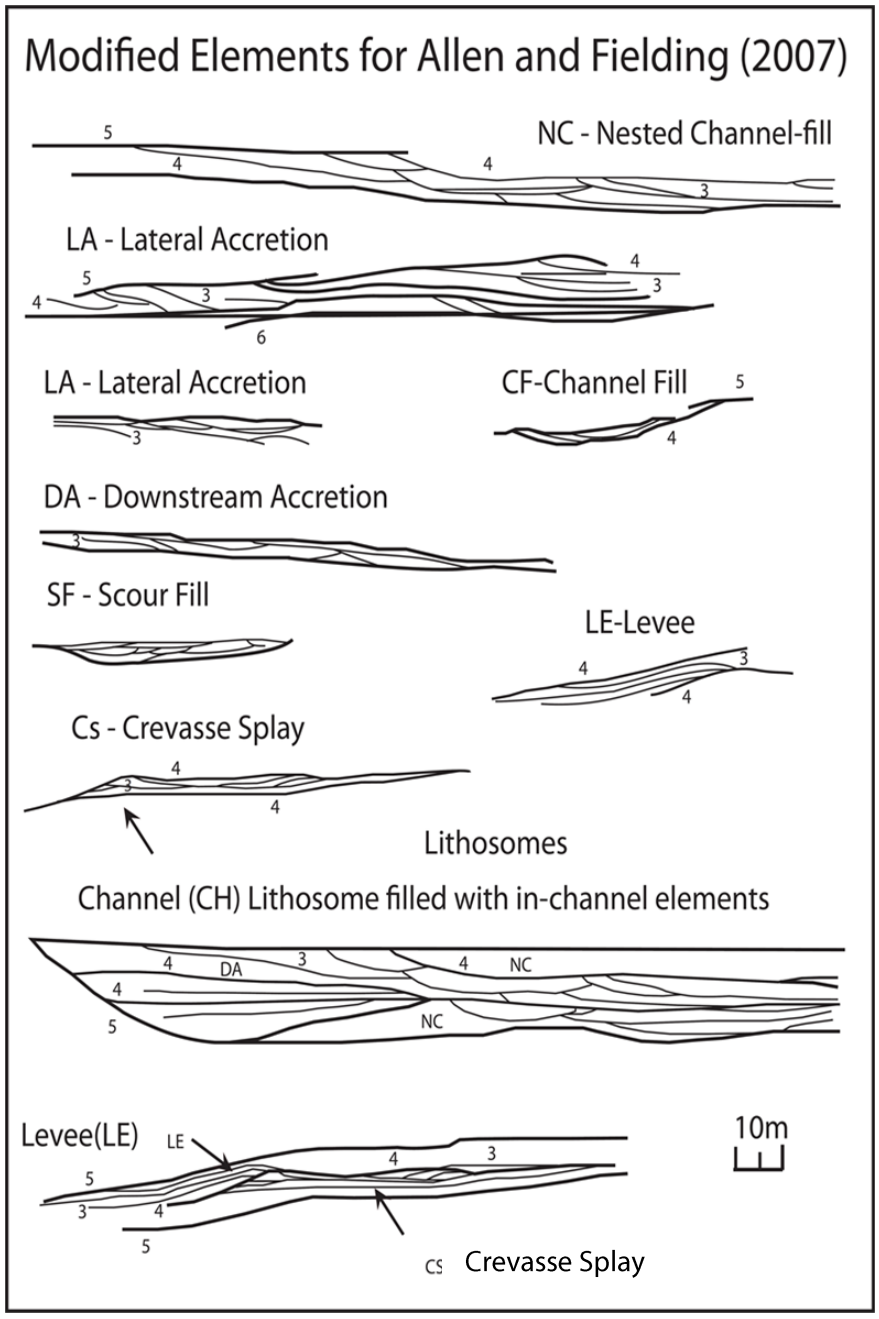

Figure 13: Basic architectural elements in fluvial deposits (modified from Miall, 1985, 1988a, 1988b).

Holbrook (2001) used architectural methods to interpret the fluvial records of the Dakota Group, their facies assemblages, and bounding surfaces (Figure 15). He also has established sets of rules that are guidelines to distinguish and classify bounding surfaces (Holbrook, 2001).

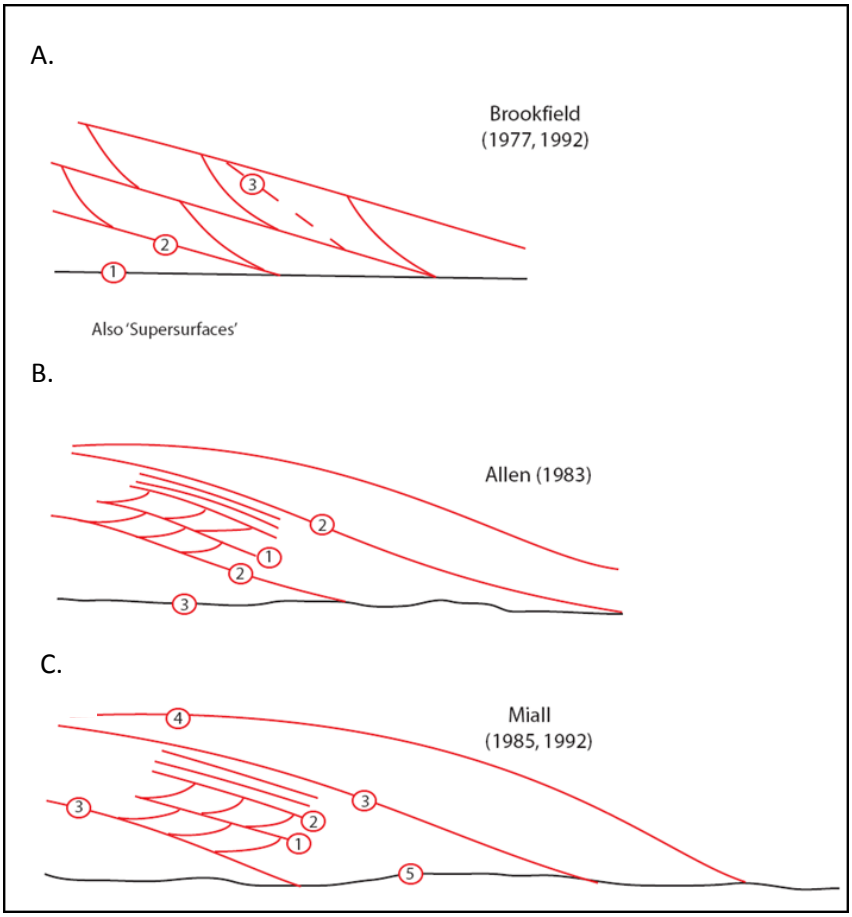

Figure 14: From the top to the bottom: (A) Brookfield bounding surface in aeolian dune. In Brookfield's method, the first-order surfaces are major laterally extensive, flat lying, convex-up bedding planes between draas. 2nd-order is low to moderately dipping surfaces bounding sets of cross-strata formed by the passage of dunes across draas. Third-order surfaces are reactivation surfaces bounding bundles of laminae within cross-bed sets and are caused by localized change in wind velocity and/or direction, (B) Allen's bounding surfaces in fluvial deposits, (C) Miall's bounding surfaces (Figure 11, 12, Table 1).

Architectural elements require bounding surfaces definition. The surface analysis method establishes lamina as the lowest bounding surface (zero), and ripple marks, small bed-forms, and first-order reactivation surfaces that bind bundle of laminae within cross-bed sets

and are caused by velocity/direction flow change. Zero and first order surfaces are bound by higher order surfaces, i.e., dune surface (mesoform or mesoscale coset) of second order surfaces. The 2nd-order is bounded by 3rd-order surfaces that cross-cut set and cosets and are enveloped by 4th-order surfaces. A point bar and levee top, or a small channel scour are typical examples of 4th-order surfaces, and occur within an encompassed 5th-order floor. In a channel stacking pattern, a channel could be captured and incised by another channel. A surface that binds a cluster of scoop-shaped 5th order channel surfaces is a 6th-order surface (e.g., channel belt). The channel (5th-order surface) should not be mistaken with 4th-order surface binding a small scour channel element (SC). Surfaces of 6th-order and higher are normally regionally extensive and traceable for hundreds of meters (e.g., Holbrook, 2001). Moreover, channel belts are bound by nested extensive surfaces and 7th-order binding surfaces. 7th-order surfaces are bound by valley fill boundaries, 8th-order. A sequence boundary, 9th-order, encompasses all the lower order surfaces and is the highest recognized order in the bounding surfaces ranks (Holbrook, 2001).

Normally larger surfaces, 7th-order and higher, record larger, allocyclic incisional events, and have been interpreted as nested valley, valley fill and regional sequence boundaries (Holbrook, 2001). In addition, the 3rd and higher orders are typically erosional, but lower-order bounding surfaces (zero–2nd) are recording a depositional hiatus (lamina, ripple, dunes and bars) (Miall, 1985). Each bounding surface is bundled by higher order rank to fit in a hierarchical or nested progression pattern (Miall, 1996; Holbrook, 2001).

There are eight basic architectural elements in fluvial deposits (Figure 13). Each element is formed by a facies assemblage and has geometry and formation time that are exclusive and separated by bounding surfaces (Miall, 1988a, 1988b, 1985; Table 1, Figure 13). Authors have expanded upon these rules and modified their definitions where needed (e.g., Allen and Fielding, 2007) and recognized that other elements maybe defined at higher levels in the architecture hierarchy (Miall, 1996; Holbrook, 2001).

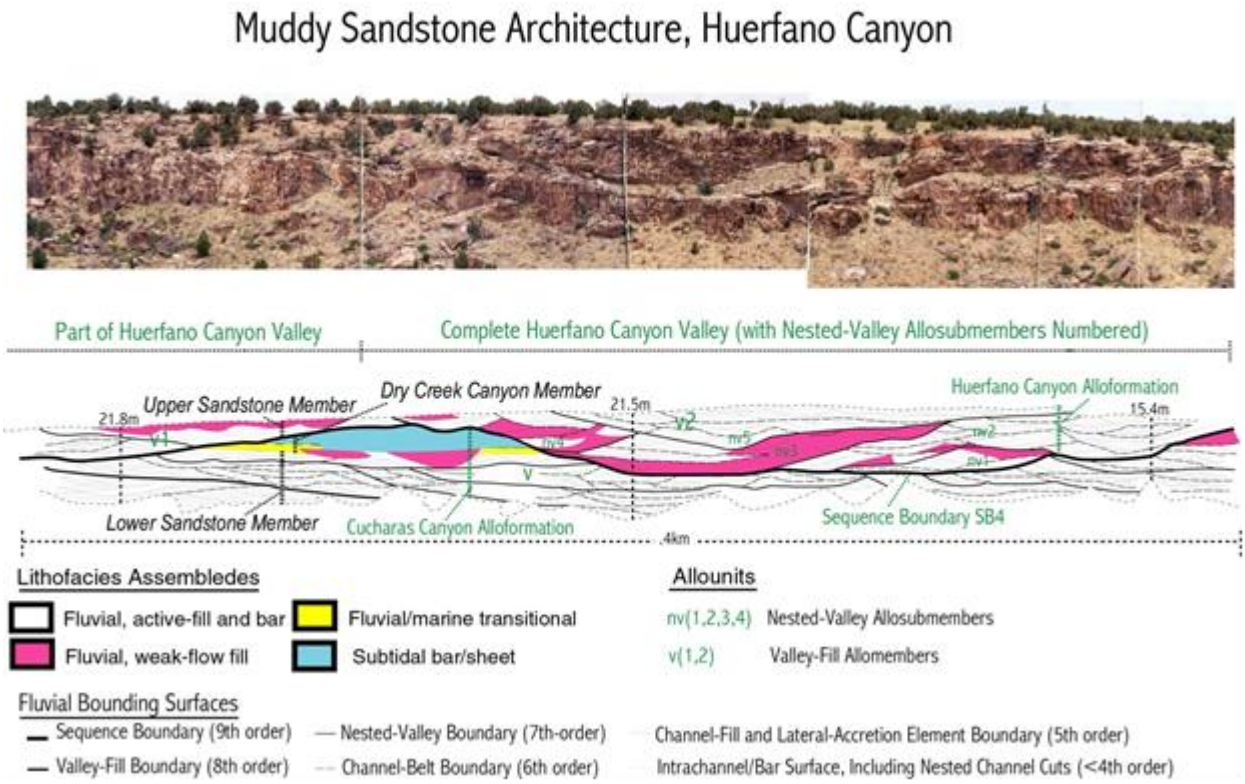

Figure 15: Interpretation of fluvial units of Huerfano Canyon using Architectural Element Analysis and facies assemblages (Holbrook, 2001).

A set of criteria and rules is used for mapping surfaces and assessing ranks from photos. Four assessments need to be applied in mapping surfaces: First, each surface is considered unique and laterally continuous until truncated or imperceptible. Second, a surface may truncate another, but surfaces may not cross. Third, any location on a surface must be younger than the material/surfaces it cuts and older than material/surfaces it binds. Fourth, lower-order surfaces will be truncated against equal or higher-order binding surfaces. Surface orders were then assigned based on guidelines. The order of a surface will be one order higher than the highest-order surface it truncates or binds. Surfaces truncate against surfaces of equal or higher ranks, and similar, but nested, surfaces maybe treated as a set of boundaries of equal orders, but the set should be ultimately bounded by a surface of higher rank. The definitions and characteristics of the surfaces are summarized in Table 1 (Holbrook, 2001).

This field work also scrutinized lithofacies, in vertical and lateral extension, based on internal sedimentary structures textures and grain sizes of any assemblages of facies. Finally, photos and drawings are merged and superimposed for interpretation. However, lithofacies are used prior to interpretation of bounding surfaces to assign and interpret architectural elements.

Analysis using architectural methodology commences with defining bounding surfaces of different hierarchies within Pennsylvanian to Permian fluvial formations of the Shafer and Canyonland basins from panoramic photos based upon Architectural Element Analysis. A series of dip and strike orientation outcrops were photographed and photos were merged for bounding surface analysis. In this research Architectural Element Analysis was applied to the FL2 fluvial interval of the Permian Cutler Group in two Shafer basin locations (Potash and Goose Neck) near Moab, Southeast Utah. The fluvial unit FL3 is the other studied section in Canyonland basin positioned to the southeast of the FL2 section and the city of Moab (Figure 2, 3, 4, and 7). Besides assigning the bounding surfaces, fluvial elements (point bars, channels, levee, etc.) and lithofacies, e.g., trough cross-bedded sandstone (St), horizontally bedded sandstone (Sh), etc., are recorded and plotted on the photos. And finally, an interpretation is applied to the FL2 and FL3 fluvial sections. The result will elucidate studied fluvial units and their depositional environment, and the factors that contributed to their formation. It also provides an explanation to how these three spatial and temporal fluvial units are influenced and characterized by up dip/down dip allocyclic climate and sea-level controls (see Appendix).

Table 2: Fluvial bounding surfaces definitions and characteristics.

First-order surface	First-and 2nd-order surfaces record boundaries within microform amd mesoform deposits. They represent crossbed set bounding surfaces. Little or no internal erosion is apparent at these boundaries, and they represent the virtually continous sedimentation of a train of bedforms of similar type. Subtle modifications in attitude, with minor erosion, maybe caused by reactivation following stage changes (Collinson, 1970), or maybe the result of changes in bedform orientation (Haszeldine, 1983b).
2nd-order surface	These are simple coset bounding surfaces. Each set is composed of set of strata (McKee and Weir, 1953). They define groups of microforms or mesoforms and indicate changes in flow directon, but no significan time break. Characteristis: Lithofacies above and below the surface are different, but the surface is usually not marked by significant bedding truncations or other evidence of erosion, except for the same kind of minor modification that occur on first-order surfaces.
3rd-order surface	These are cross-cutting erosion surfaces within macroforms that dip at a low angle (normally < 15 degrees) and truncate underlying crossbedding at a low angle. They may cut through more than one crossbed set. They are commonly draped with intraclast breccia. Facies assemblages above and below the surface are similar. Third order surfaces may also develop at the top of minor bar or bedform sequences, and are draped by mudstone or siltstone, indicating lower discharge. Succeeding strata commonly contain a basal intraclast breccia composed of rip-up clasts of the draping fine-grained sediments. Other characteristics: These surfaces indicate stage changes, or changes in bedform orientation within the macroform. They indicate a form of a large "scale reactivation" (Collinsons,1970).
4th-order surface	These surfaces represent the upper bounding surfaces of macroforms. They typically are flat to convex-upward. Underlying bedding surfaces and first-to-third-order bounding surfaces are truncated at a low angle or maybe locally parallel to the upper bounding surface, indicating they are surfaces of lateral or downstream accretion. Mud drapes on the element underlying the surface are common. Similarities and differences between 4th and 3rd-order surfaces: These surfaces are defined when architectural reconstruction indicate the presence of macroforms, such as point bar or sand flats. The best clue to the presence of 3rd-and 4th-order surface is their gentle depositional dip. Differences: The best way to distinguish these surfaces from each other is to note whether the lithofacies assemblages above and below the surfce are different, indicating a change in element (macrofom)type, Miall (1989).
5th-order surface	Surfaces bounding major sand sheets, such as channel-fill complexs. They are generally flat to slightly concave-upward, but they maybe marked as local cut-and-fill relief and by basal lag gravels. 5th-order of Miall is of 3rd-order of Allen, and "major" surface of Bridge and Diemer (1983).
6th-order surface	Surfaces defining groups of channels, or paleovalleys. Mappable stratigraphic units such as member or sub-members are bounded by 6th-order surfaces. 6th-order surfaces are Not defined by Allen(1983). Both 5th-order and 6th-order surface are easiest to map because of their wide lateral extent and essentially simple, flat, or gently curved, channelized geometry.
7th-order surface	It's a surface the compass channel belts. Nested valleys ('nv' allosubmembers: (7th-order) (Holbrook, 2001).
8th-order surface	Valley fills ('v' allomember): (8th-order)(Holbrook, 2001). There are two types of erosional unconformities: Broad planar erosional surfaces that form during relatively slow sea-level fall. Incised-valleys that form during relatively rapid sea-level fall. (Strong and Paola, 2008).
9th-order surface	Sequences (alloformations): (9th- order) (holbrook, 2001). A surface separating younger from older strata along which there is evidence of subaerial erosion and truncation and subaerial exposure and along which a significant hiatus is indicated "Van Wagoner" (1988).

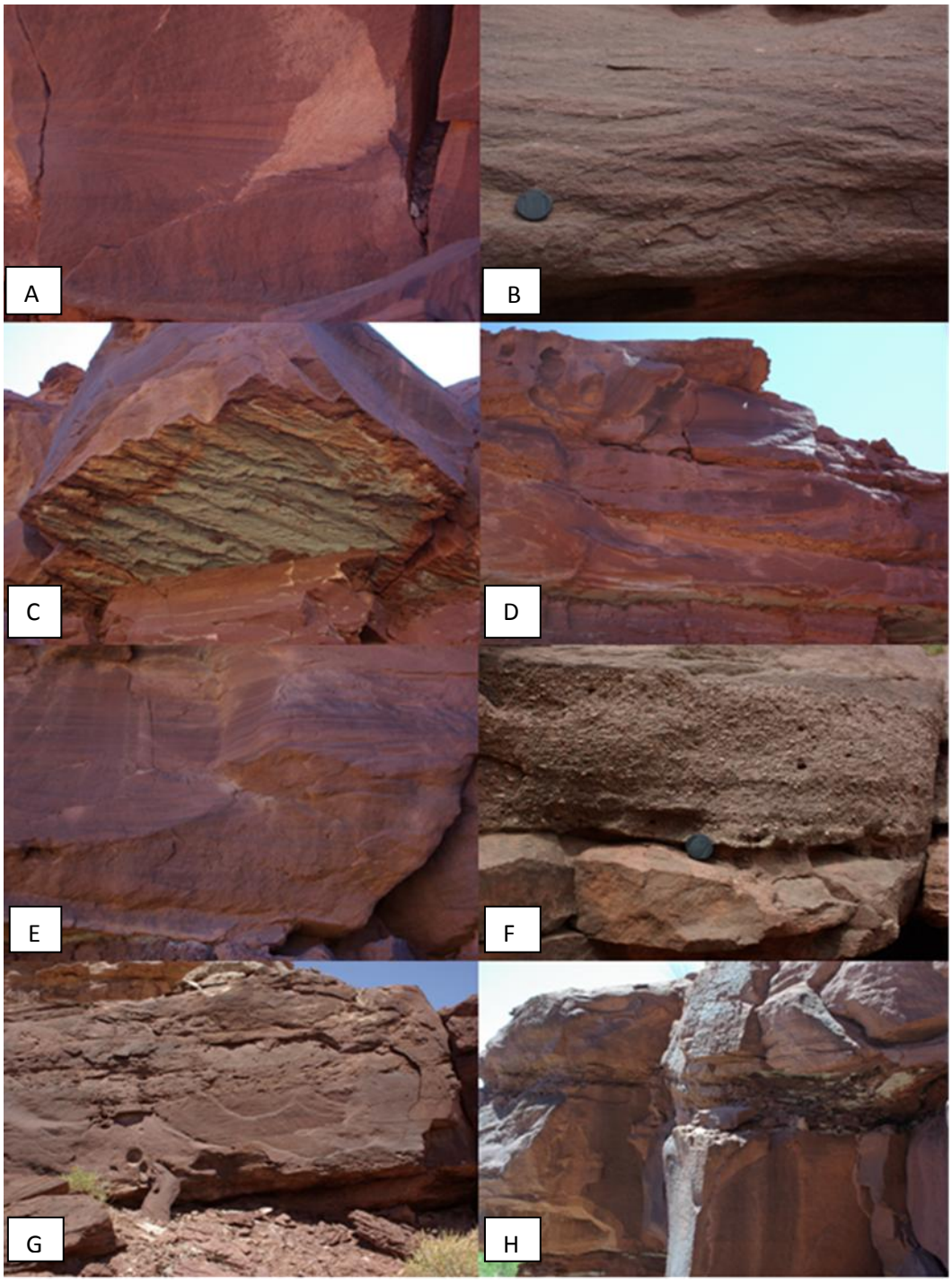

Figure 16: Observed facies in the Shafer basin, Utah. From the top left to the right: (A, B) trough cross-bedded fluvial deposits, (C) erosive scours (sequence boundary) at the bottom of the extensive fluvial rocks - base of the FL2, (D) incising channel into underlying sand dune, (E) laminar fluvial sand sheet, (F) pebble and conglomerate fluvial bed(g) trough cross-bedded fluvial medium to coarse sandstones (Canyonland), (H) stacking multi-story channels (Canyonland).

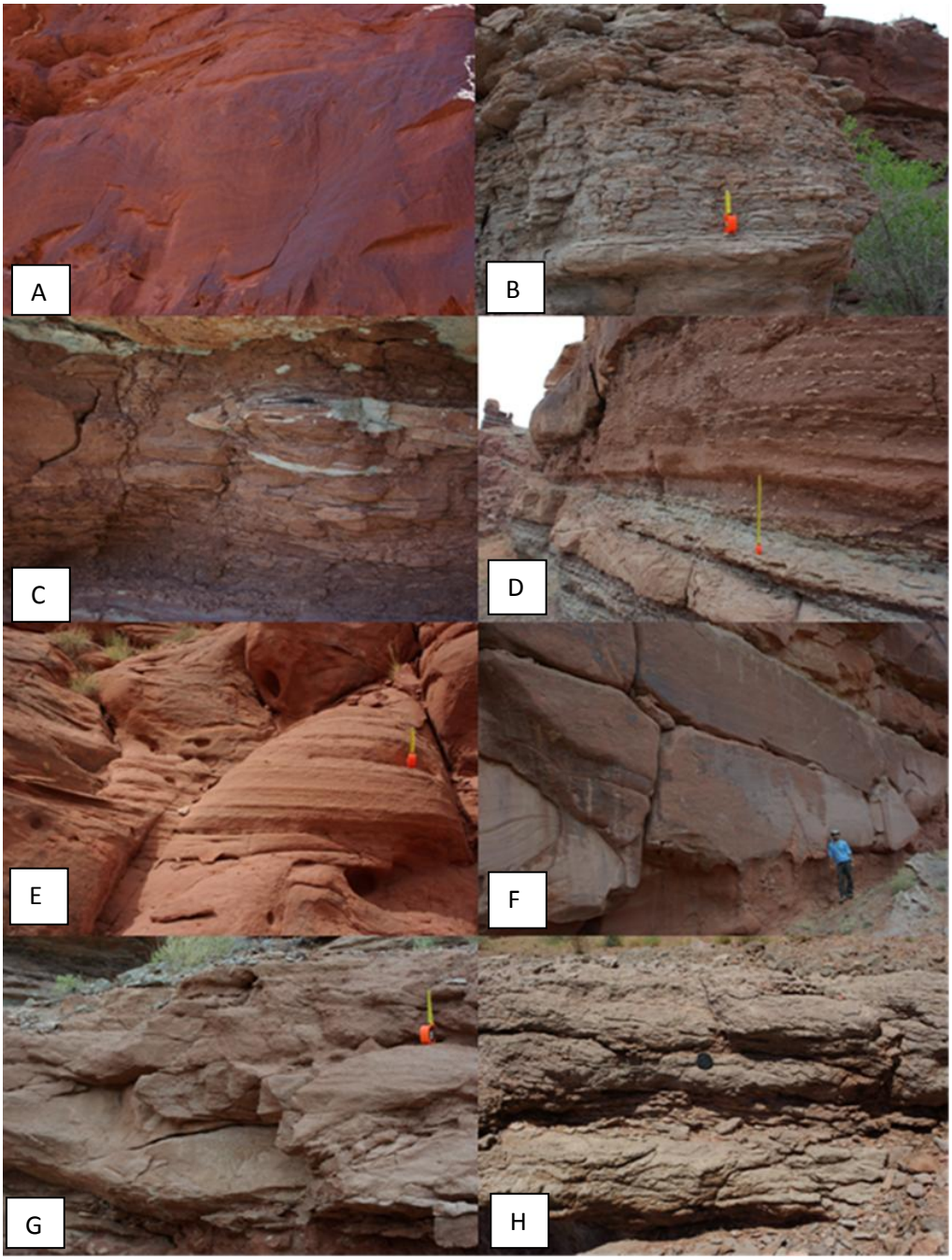

Figure 17: Observed facies in the Shafer basin, Utah (from the top left to the right): (A) fluvial convoluted bed, (B) paleosol, (C) fluvial overbank deposits, (D) marine limestone underlying immature paleosol, (E) planar cross-bedded sand sheet dunes, (F) massive sandstone dunes, (G) shore current marine grainstone, (H) Cedar Mesa limestone.

CHAPTER 3

DATA/RESULTS

The study of fluvial units of the Lower Cutler beds has been divided in this study based on their location within the Shafer basin into: (1) Potash, (2) Goose Neck, and (3) Canyonland locations.

3.1 The Potash location

There are several paleo-current measurements that indicate dominantly a SW direction for fluvial units, extending from the previously existing Uncompahgre uplift to the paleo-shore line (FL2, FL3); however, there are a few NW paleo-current directions as well (Figure 18 and 19).

A.

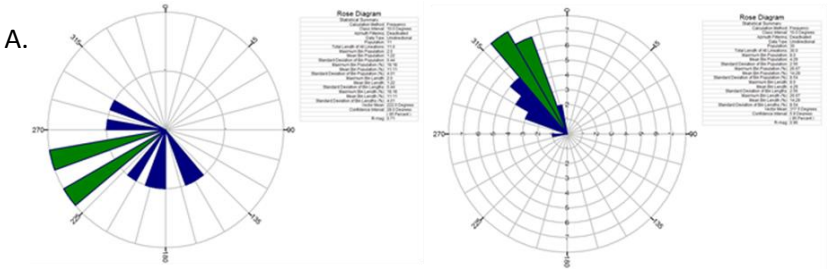

B.

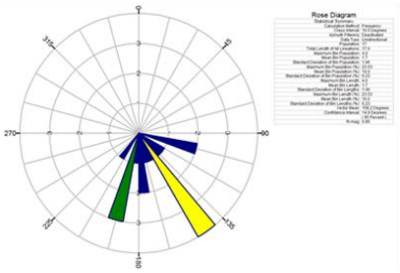

Figure 18: (A) Rose diagrams showing paleo-current direction of the FL2 of the Shafer basin (Potash) only. Left diagram showing general paleo-current direction of all fluvial units of the Lower Cutler beds that varies from SE to NW (blue color represents mean direction of the paleo-direction). Right diagram shows general direction of FL2 of the Shafer basin (Potash) dipping at a W-NW direction. Note discussion of variation among paleo-current direction. (B) The rose diagram showing general direction of aeolian sand dunes of Lower Cutler beds in the Shafer basin (Potash). Note the mean SE direction of paleo-currents from sand bodies (Blue = mean ± 1 Standard deviation (Sd), Green= mean ± 1-2 (Sd), Yellow = mean ± 2-3 Sd).

Paleo-current direction

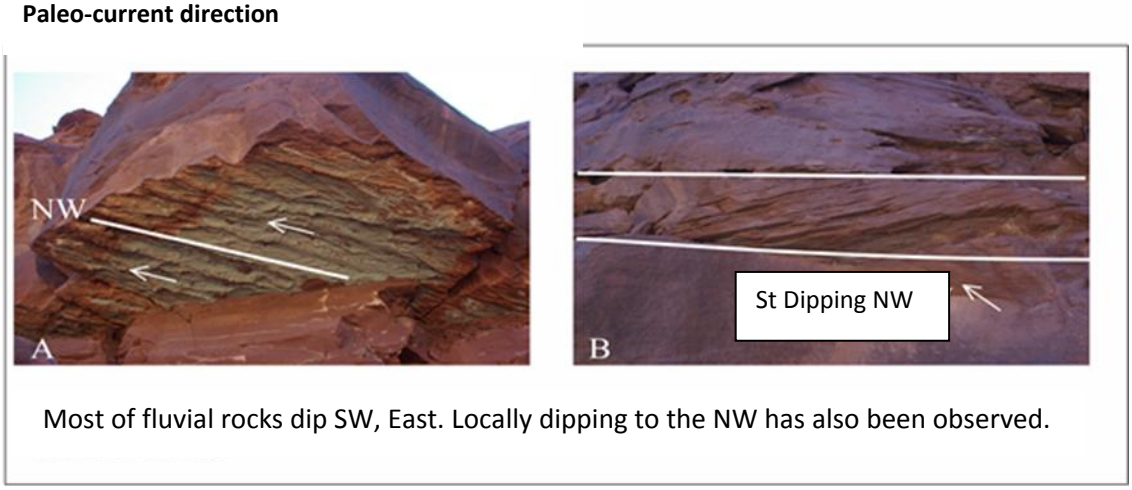

Figure 19: At many localities FL2 unit in the Potash location showed NW paleo-direction that is at odds with the general SW direction.

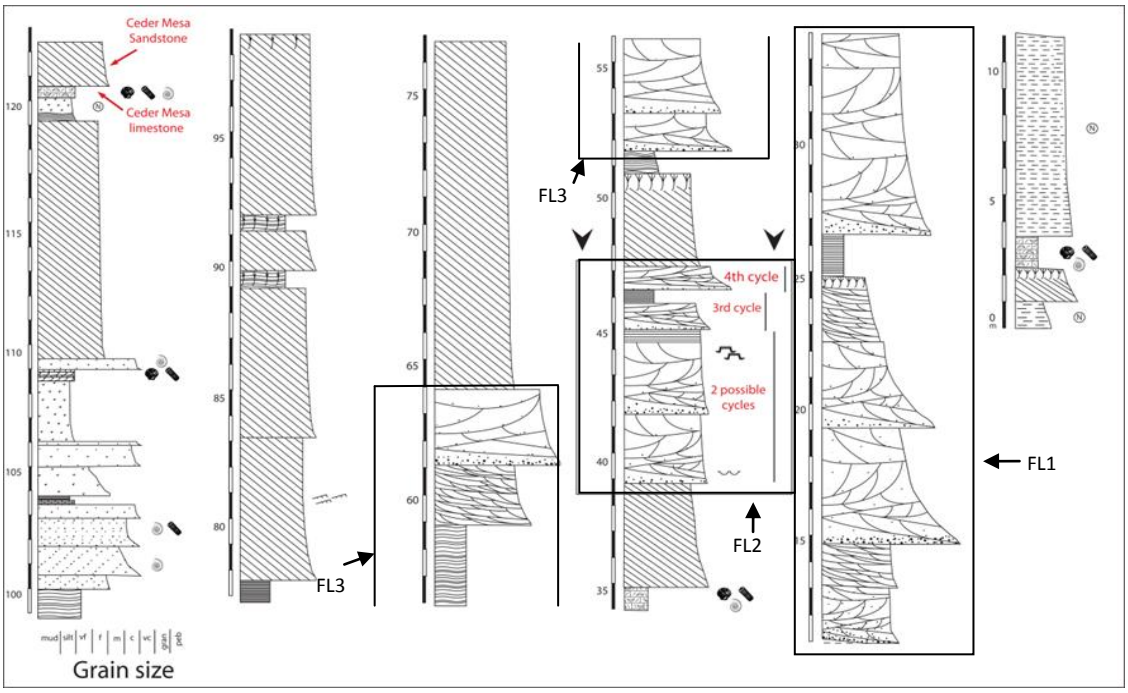

Figure 20: Stratigraphic cross-section of Lower Cutler beds in Shafer basin (Potash). Fluvial unit enclosed by a square is FL2 fluvial unit. FL2 shows 4 fluvial stories/cycles and is bounded by aeolian dunes. The Cedar Mesa limestone/sandstone is marked by red arrows (top left).

.

Two sections are studied in the Lower Cutler beds in the Shafer Basin (Potash) with respective dip and strike orientations (see Appendix). Trough cross-bedded sandstone (St) is the dominant lithofacies, however, horizontally bedded sandstone (Sh) can be seen as well. DAB is a boundary that marks lithofacies changes from flat and wavy sand-sheets (Sh) to trough cross - bedded sand-waves (St). Similarly, the FIV surface punctuates the abrupt change in direction (SE to SW paleo-current change), lithofacies, and transport agent (windblown sand-sheets to fluvial deposited bars) (Figure 21, B and D).

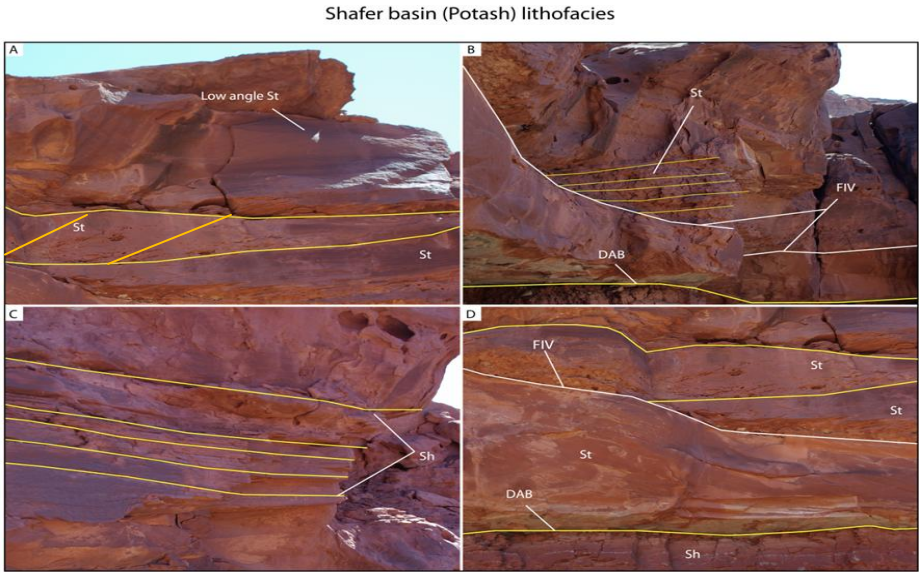

Figure 21: Shafer basin (Potash) fluvial lithofacies are in the order (A) Trough cross-bedded within lateral accretion bars (LA). (B) DAB (dry aeolian/interdune boundary) is the base of aeolian dune (yellow line); FIV is the base of the FL2 unit presented as a sequence boundary surface. The trough cross-bedded at the base is in strike orientation. (C) Horizontally bedded sandstone (Sh) reflects the increase in hydraulic velocity within the first fluvial story. (D) is the dip view of the Section B. Note the lowermost unit (Sh) which represents damp surfaces of aeolian interdune.

3.2 The Goose Neck location

The Shafer basin fluvial unit near the Goose Neck location by the Colorado River loop has a very similar vertical pattern to the Lower Cutler beds in the Potash location. It is based by a fluvial incision into dry aeolian sandstone and is topped by another aeolian sandstone. The unit FL2 retains stacks of fining upward sediments with scours separating the unit into three cycles (Figure 22, 23 and 24, see Appendix).

In the vertical section limestone passes upward into paleosol and interdune, then aeolian dune. The FL2 unit cuts into dry aeolian sand and even into the underlying paleosol-interdune section (Figure 22).

The FL2 facies in the Goose Neck location are trough cross-bedded sandstone (St), horizontally bedded sandstone (Sh), and planar cross-bedded sandstone (Sp) (Figure 23 and 24, Appendix). A paleo-current direction is not available.

In this location, at least three separate fluvial elements are identified: lateral accretion bars (LA), channel fill (CH), and floodplain deposits (FF), (Figure 25, and Appendix).

The second fluvial cycle is marked by a paleo-river incision into the overbank fines of the first cycle. The concave up erosional surface incised deeply into the lower bars and deposited coarse grained sediments at its base. The second cycle encompasses several migrating accretion bars within channels that at times were incised by other channels. The second cycle is aggrading and seemingly has created a nested or channel amalgamating pattern (Figure 25). The third cycle is represented by migrations of several trough cross-bedded, mid-channel/macroform bars downstream in a channel belt or nested valley.

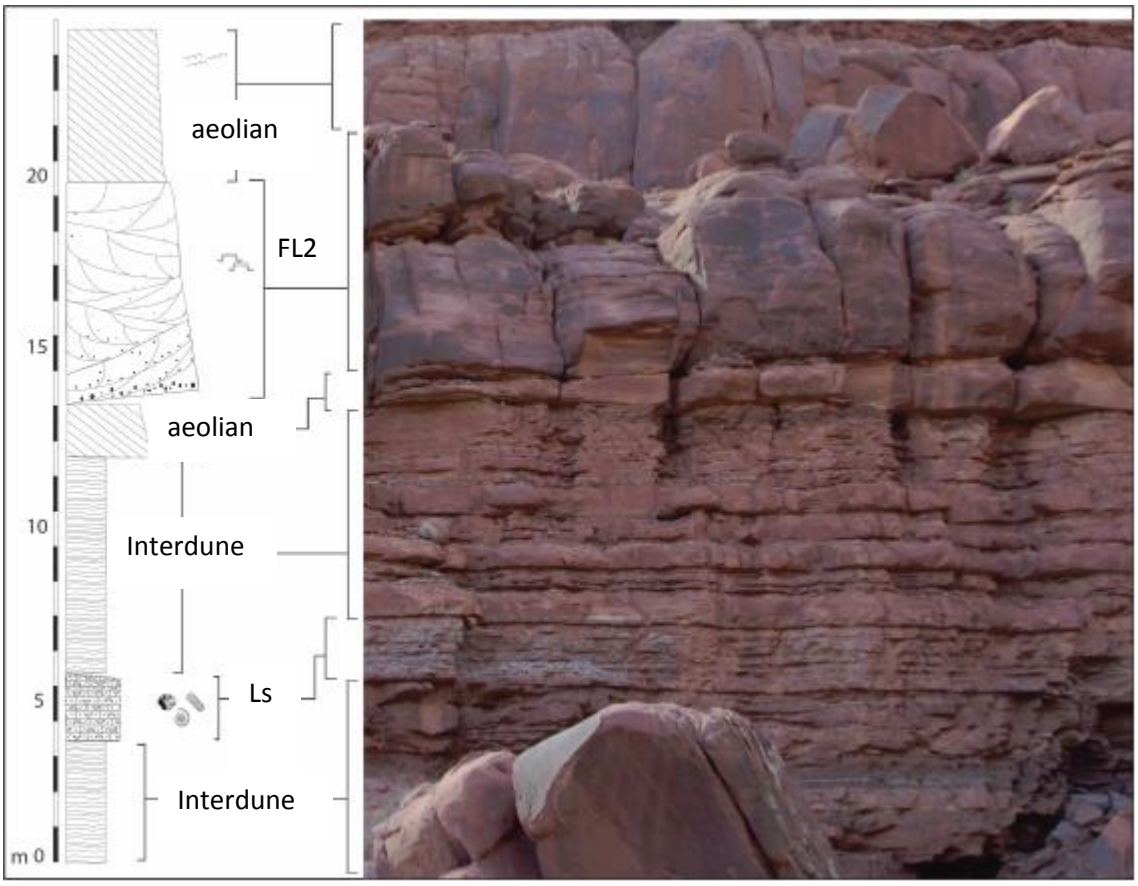

Figure 22: Stratigraphic cross-section of the Lower Cutler beds in the Shafer basin (Goose Neck location). The vertical section on this photo confirms the large size of fluvial unit FL2 that is underlying dry aeolian sand dune. Note how the lower aeolian sand is pinching out to the Southwest (left of photo).

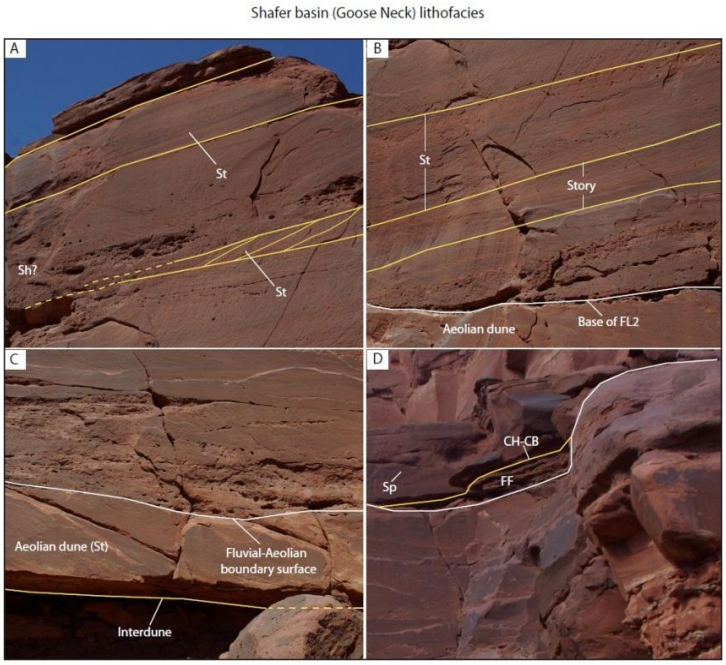

Figure 23: Goose Neck Fluvial unit in the Shafer basin (Lower Cutler beds, dip direction). Majority of lithofacies in this section are trough cross–bedded (St), horizontally bedded sandstone (Sh), and some planar cross - beds (Sp).

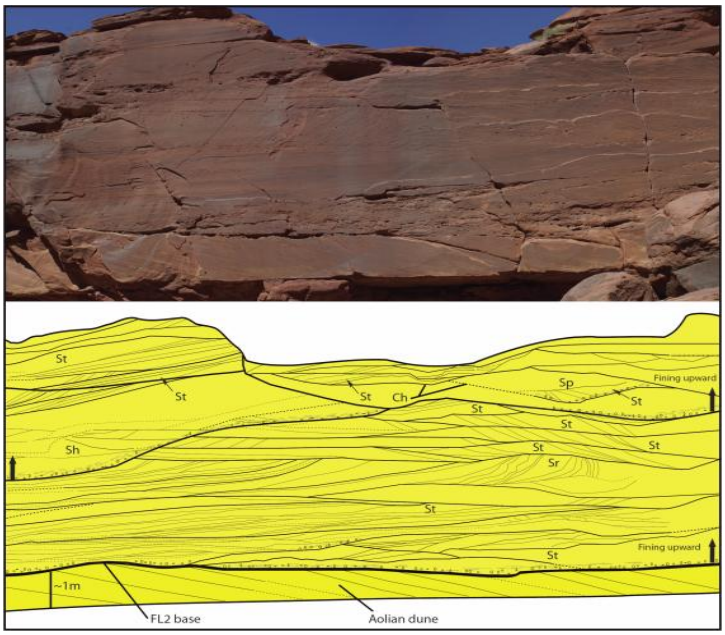

Figure 24: The FL2 has incised in the lower aeolian unit below, and aggrades till incised by second fluvial cycle (arrow). The second cycle maybe a terrace complex surface, or a channel belt (arrow on the left side of the photo. Also see notes in discussion). The third cycle channel belt has incised into the second cycle creating a vertical stalking of channel belts. Note the first cycle thickness that characterizes several stories of trough cross-bedded lateral accretion bars.

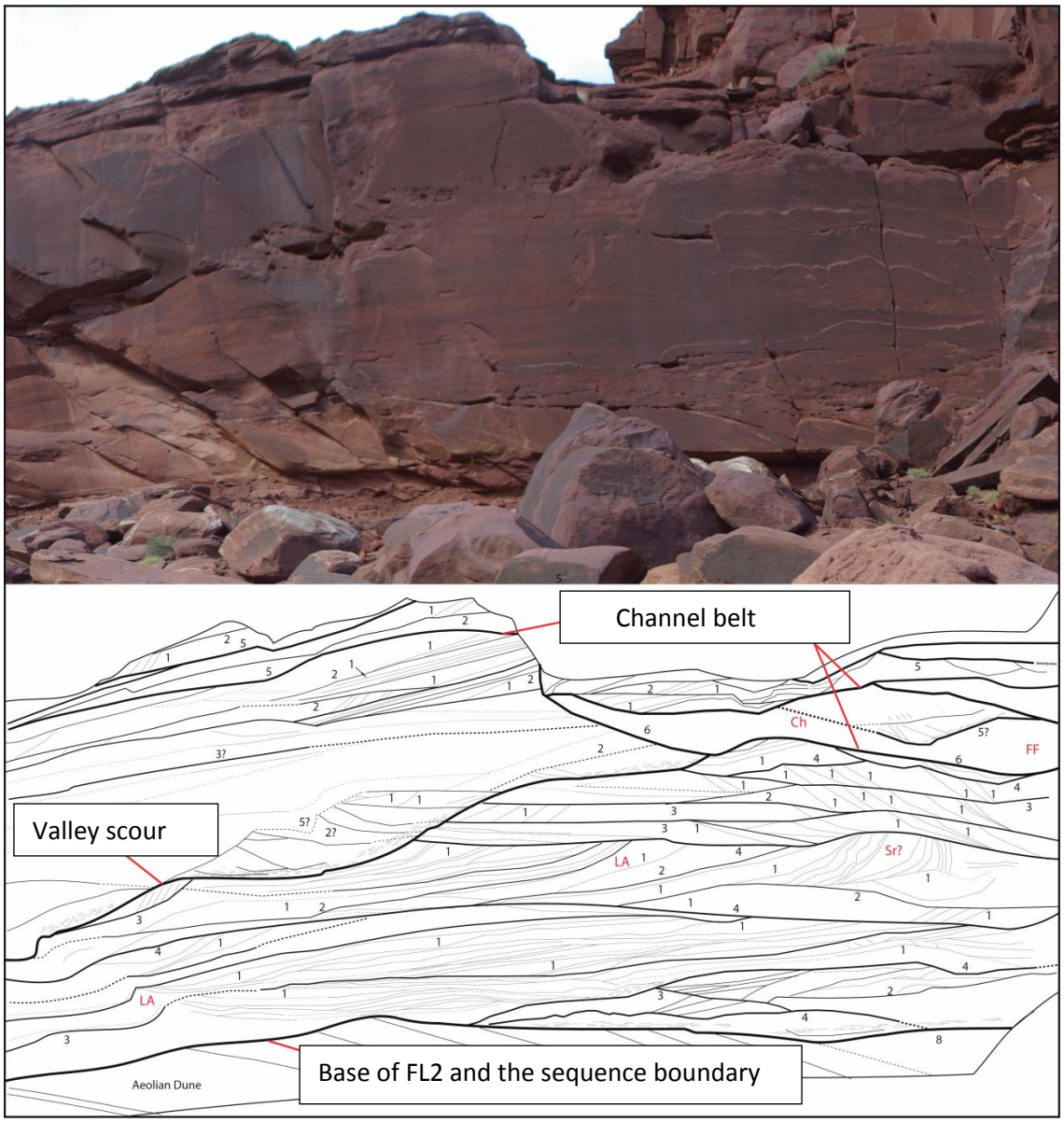

Figure 25: Fluvial deposits of the Shafer basin (Goose Neck). The fluvial unit has incised into an aeolian sand dune. The first fluvial unit aggrades up to few meters height and gets incised by a terrace or a channel belt. The third fluvial incision would be of a channel belt or higher. In this figure architectural elements such as LA (lateral accretion bars), SG (sediment gravity flow), FF (overbank fine) are observed. Bounding surfaces include a valley fill boundary at the base of the FL2. Surfaces 1-4 orders occur within a channel. Channels are 5th-order surfaces that maybe bounded by a channel belt 6-order surface. Note: refer to Table 1 for more information about surfaces classification.

3.3. The Canyonland location

The Canyonland Upper Paleozoic fluvial unit represents the uppermost fluvial excursion into the Lower Cutler beds (FL3). The Canyonland fluvial unit represents at least two channel belt cycles within the cross-section. Yellow lines represent the channel belt surfaces (Figure 26).

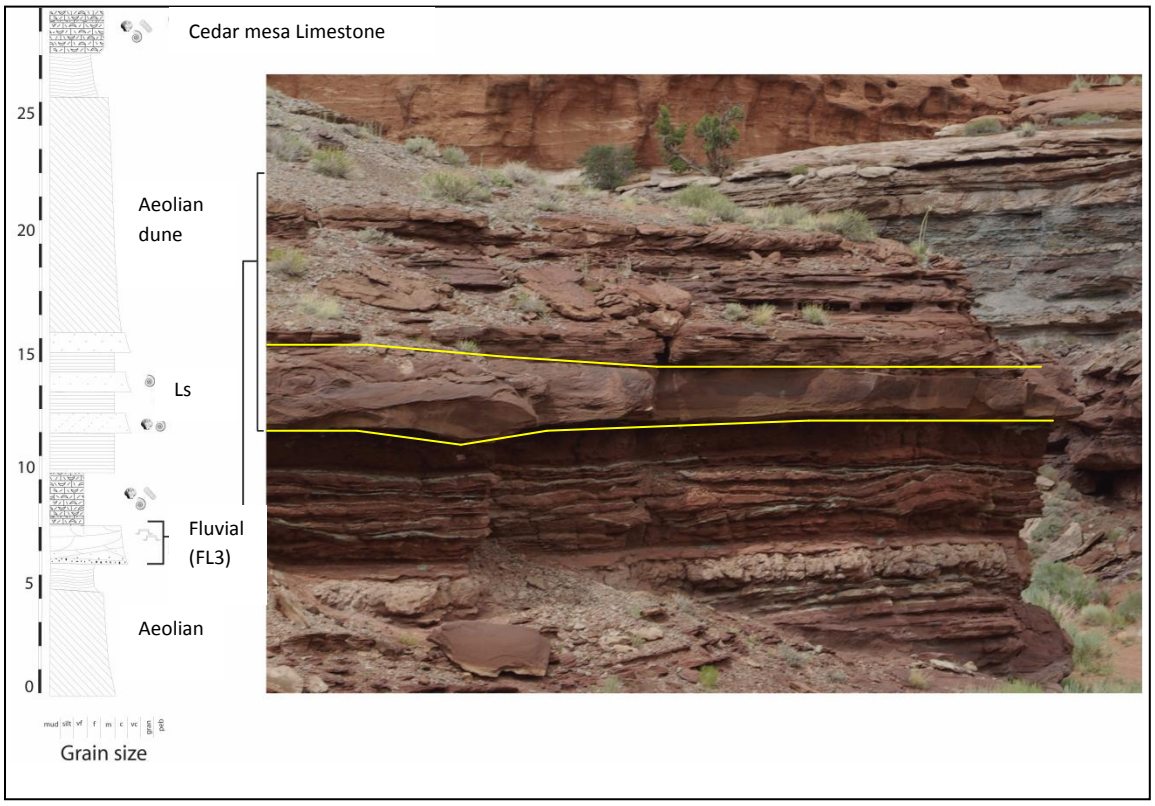

Figure 26: The Canyonland fluvial unit is the uppermost layer in the photo. It is recognized by trough cross-bedded sandstone (St) within downstream accretion bar (DA). It is incising into dry aeolian dune beds and is overlain by a very thick interbedded bioclastic, grainstone and carbonate mudstone. These transgressive limestone beds are visible to the right of the photo (grayish bluish). The uppermost Lower Cutler beds fluvial unit represents a multiple of complex braided/meandering stacking channel belts.

The base of the measured cross-section is aeolian dune sand approximately five meters thick, underlying interdune strata. The fluvial unit of three meters thickness fines upward

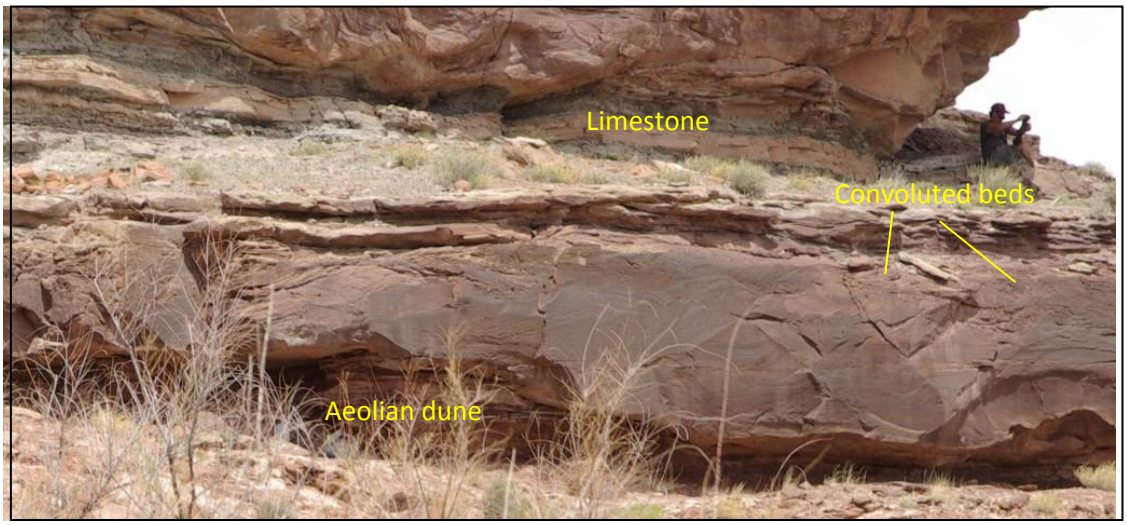

Figure 27: Paleozoic fluvial unit in the Canyonland basin is underlain by aeolian dune and overlying by marine limestone.

into completely chaotic and convoluted beds. Convolution and convoluted beds are most common in the top of fluvial unit and the top of the fluvial unit is capped by marine limestone (Figure 27).

Pebbles mixed with fine to silty beds are at the base of the studied fluvial unit in the Canyonland basin. The fluvial incision into interdune strata has the same style incision of underlying rocks as FL2 in the Lower Cutler beds of the Shafer basin in the Potash location; however, sediments here are finer.

Lithofacies are trough cross-bedded sandstone (St), horizontally bedded sandstone (Sh), and convoluted bedded structure (Cv) within channel belt fills (Figure 28). Paleo-current measurements and directions were not collected.

The Canyonland fluvial deposits are composed of several architectural elements such as lateral accretion bars (LA), mid-channel bars, and channel fill elements (CF) (see Appendix for more details). Likewise, the Canyonland basin section is composed of several stacked channel

belts that each has incised and aggraded till the incision of the next overlying channel belt. In addition, each channel belt may encompass a channel that is filled with either an accretion bar element (LA) or channel fill element (CF). The base of FL3 is bound by a sequence boundary. The top of the FL3 unit is charactorized mainly by convoluted bedded sandstone (Figure 29 and 30).

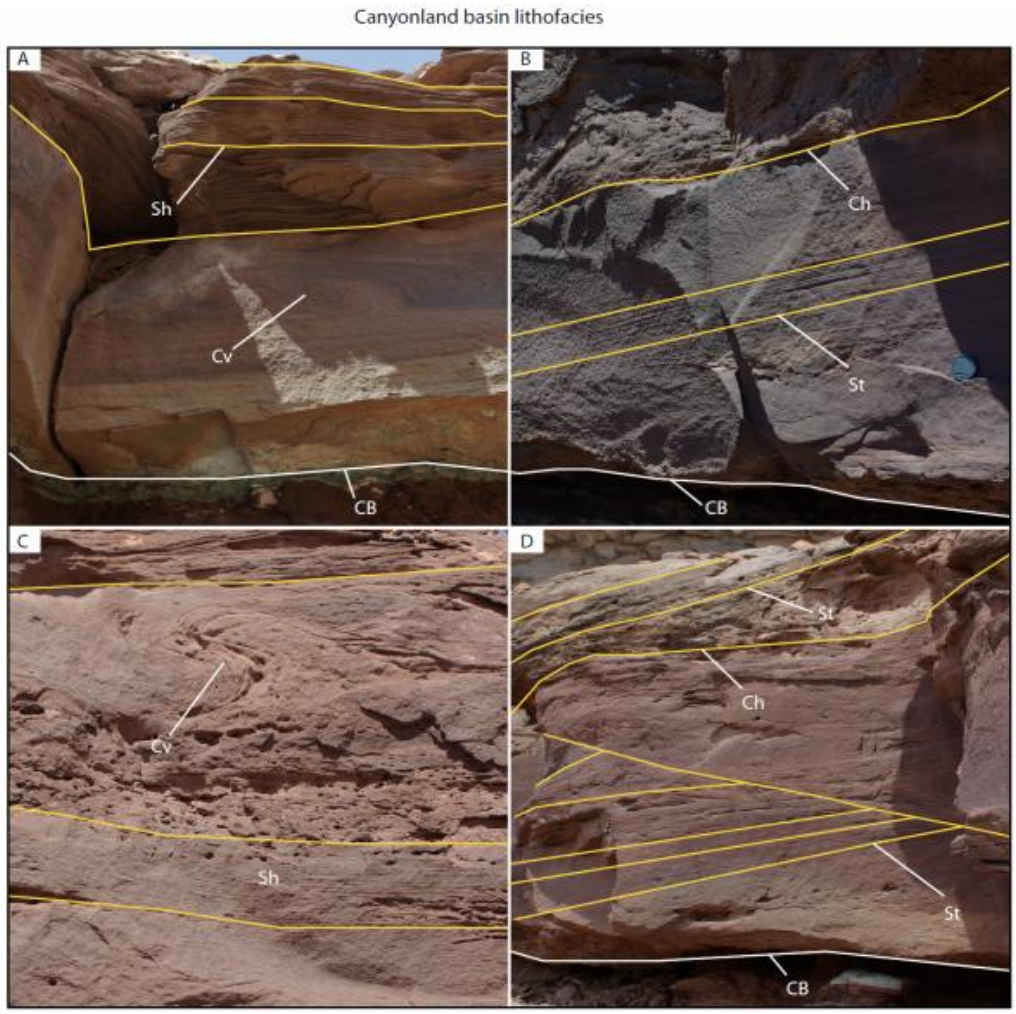

Figure 28: Observed lithofacies in the Canyonland fluvial unit. (A) A horizontally bedded sandstone (Sh), A convoluted–bedded sandstone (Cv), the sequence boundary (Sb). (B) A trough cross–bedded sandstone (St), and a channel fill (Ch). (C) A convoluted–bedded sandstone (Cv), and a horizontally bedded – sandstone (Sh). (D) A trough cross–bedded sandstone (St), a channel (Ch), and the sequence boundary (Sb).

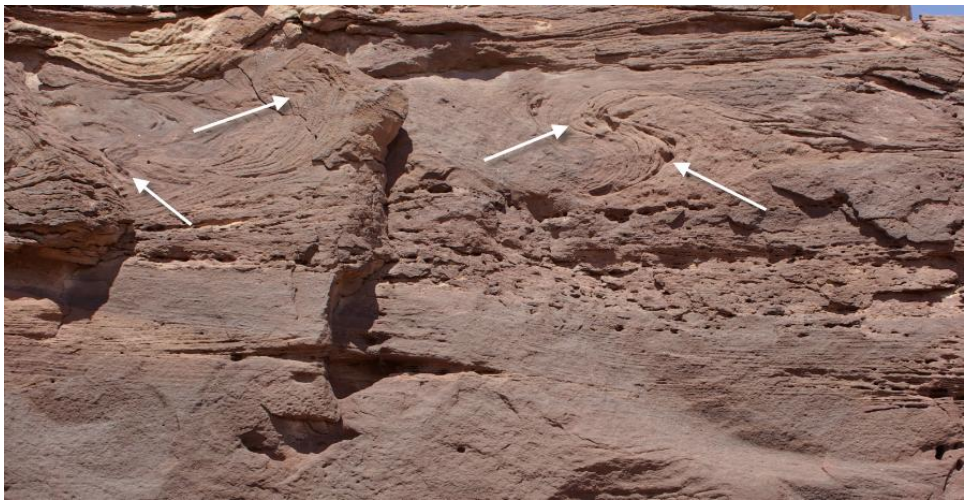

Figure 29: FL3 fluvial unit that is highly affected by convoluted bedded sandstone (Cv-white arrows) in the uppermost part of the channel belt.

CHAPTER 4

DISCUSSION

This study builds on the macrostratigraphy of two stratigraphic fluvial units (FL2 and FL3) confirmed within the Lower Cutler beds in the Shafer basin and defined by previous authors (Jordan and Mountney, 2010). The fluvial unit FL2 was studied in the Potash and Goose Neck locations, whereas FL3 was studied in the Canyonland location (Jordan and Mountney 2010). This research also compares the Lower Cutler beds fluvial units in the Shafer basin (Potash and Goose Neck) location (i.e., FL2) with the Canyonland fluvial unit (FL3) with respect to fluvial architecture and depositional environments.

4.1 The Potash location

The fluvial Lower Cutler beds in the Shafer basin exhibit a fluvial system that aggraded above a sequence boundary. The boundary extends for at least 65 km (Jordan and Mountney, 2010), 3.7 km of which were examined for this research in the Shafer basin. This fluvially scoured sequence boundary has completely removed the underlying aeolian sand at many locations and is juxtaposed directly above lower interdune beds.

Dip oriented trough-cross sets from migrating dunes within lateral accretion bar elements (LA), are at the base of the FL2 unit in the Potash location. The upper part of the basal lateral accretion bar is cut by another large extending surface that is of a terrace order that encompasses several amalgamated small channels or bar surfaces. The absence of overbank deposits suggests their potential removal by incision of the higher order surface that starts the next fluvial aggradational cycle. The nested channels in the second cycle are incised by trough cross-bedded braid bars of the third cycle (Potash dip direction, see Appendix).

The Lower Cutler beds lithofacies of FL2 section in the Shafer basin incise blown sand-sheet to interdunes. The FL2 fluvial unit aggrades to aeolian sand waves and other lithofacies

(Figure 20). The Cedar Mesa limestone represents the upper boundary of the Lower Cutler beds (Figure 17).

The paleo-direction of rivers in the FL2 unit of the Potash location was from northeast to the southwest (Terrell, 1972; Mack, 1977; Jordan and Mountney, 2010). However, this research has recorded several NW paleo-direction trends of the FL2 unit (Figure 18 and 19). To describe this inconsistency, these fluvial bars may have been deposited south-southwestward but tectonically have been rotated 45 degrees to the north later (Condon, 1997). Alternatively, paleo-current discrepancies among bars and stories may reflect either local tectonism or nodal avulsion (Gibling, 2006). Due to the inaccessibility of the Goose Neck unit, paleo-current measurement was not possible.

Lateral accretion elements derived from migration of 3-D side-attached bars are dominant in the lowermost section of the FL2 unit in the Potash location. The channel element (CH) is almost absent from the lower part of the unit. However, channels are abundant in the middle to upper section of the unit. This observation affirms the local change from less channelizing, stable to more channelizing, smaller and more complex bars and channels reflective of a transition to more braided and/or smaller straight rivers with less large lateral attached bars (Figure 3). This transition compounds with each phase of incision within the FL2 sand sheet. These mid-bars are incising and stacking secondary channels (see Appendix; Dip direction).

The studied FL2 section in the Shafer basin (Potash, strike orientation) shows three valley scours in which each has nests of several channel belts. Troughs of cross-bedded sandstone (St) are the most dominant facies. Channel element (Ch) and Nested channel fill (Nc) are the only elements that were apparent (Appendix). Lack or absence of overbank deposits maybe interpreted as incision of the upper braided channel belt into the mixed meandering/braided lower channel belt by paleo-rivers that constantly cut and filled during overall aggradation. The clear transition from thick and large stable channels producing large

bars to smaller channels and/or braid systems is not as apparent in this orientation. Channel belts of the lower cycle are more vertically amalgamated and the preserved part is thinner.

4.2 The Goose Neck location

The FL2 unit stratigraphic section is approximately six to over eight meters thick in the Goose Neck location and has deposited pebble/coarse grains at its base. It is partitioned by two extensive surfaces that are terrace or valley boundaries that split the section into three cycles (Figure 24, 25 and Appendix).

The first cycle of the FL2 unit is formed by several layers of low-angle trough sets interpreted as parts of large lateral accretion bars elements that have incised into aeolian dunes. The medium-order bounding surfaces (3-4) of the lateral accretion bars appear to be large and flat on strike orientation. The formation of stories of small channel above these surfaces would be consistent with chutes on a large mid-channel or a point bar of a sizable river. Each stacked (LA) bar fines upward until cut by an extensive fluvial valley surface of a second cycle (Figure 24 and Appendix). The second cycle is aggrading and filled with what seems to be a stacking of near flat mid channels bars that cut the accretion point bars within the same cycle (Figure 24, 25 and Appendix). This structure shows a major change in the fluvial system along with a new cycle of valley incision and aggradation (c.f., Holbrook et al., 2006). Moreover, the third cycle formed by cutting of the second cycle's top followed by the stacking of large trough cross-bedded bars based by a bounding surface of nested valley/valley size order. Architectural elements of the FL2 in the Goose Neck locations include channel element (CH), lateral stories of lateral accretion bars (LA), and trough cross-bedded mid channel bars (DA). Channel elements (CH) are fills of secondary (bar top) and primary (bar lateral) channels in a dominantly braided river system. Nonetheless, having large stacking lateral point bars in the first, and partly in the second cycle, supports FL2 formation by a mixed braided/meandering river system. The strike orientation channels or channel belts appear to be laterally flat or possess low angle dipping surfaces.

Valley incision might be as a consequence of changing equilibrium gradient because of variation in balance of discharge and sediment supply. Temporarily increased discharge could cause channel incision. Conversely, more sediment could have been derived from the Uncompahgre uplift to cause aggradation after incision. The incision into lower fluvial units and the lowering of the base level may have formed reincision of aggrading fluvial deposits preserved as the higher order surfaces that partition FL2. From cross-section stratigraphy, the Shafer basin FL2 unit underlies several tens of meters of continental aeolian and interdune deposits indicating a change in climate and no indication sea level rise (Loope, 1985). This phenomenon is in contradiction with the general back-stepping filling processes which occur with a flooding of the terraces and valley fills with constant sea-level rise and sediment supply in deltaic regions (Rodriquez et al., 2005). This process suggests that terraces exhibit the cut and fill and record changes in the balance of sediment and river discharge during an overall aggradational trend well up dip of the strand, rather than indicate discrete base level rises and falls associated with transgression and regression. The paleo shoreline would have been too far from the FL2 unit location for sea-level shift to have controlled or changed the base level.

Based on the Architectural Element Analysis of the FL2 unit (both locations), it can be inferred that mobile channel belts deposited their narrow to broad sheets (c.f.,Gibling, 2006) through unconfined braided systems that fed paleo coastlines much farther down dip (Jordan and Moutney, 2010). A single thread meandering river, however, may produce sheet-like sandstone if subsidence is low and if avulsion frequency and rates of channel migration are high (e.g., Holbrook and Schumm, 1999).

Siliciclastic sand (medium, fine) is the main sediment grain for fluvial units in the Potash and the Goose Neck locations. The FL2 unit in the Potash location has grains ranging from some pebbles at the base to medium sand and fining upward. Siltstone and mudstone are completely absent. However, this research has documented a remnant of the floodplain section (silt, mud) that had existed but has been incised and removed by overlying fluvial bars (Figure

23, D). A deep incision well beyond the depth of a channel belt into the flood plain in an aggraded valley fill and its removal has created a valley sized boundary (Figure 25, and Appendix)

Low vegetation, high precipitation and delivery of large quantities of bed load, or interaction of increasing slope and great discharge (e.g., Leopold and Wolfman, 1957; Schumm, 1968), have produced FL2 braided fluvial architecture. Channel bars not exceeding one meter in height indicate local and temporal deposition under shallow water. The last fluvial cycle in the Goose Neck location (Figure 25), however, represents thick downstream accretion bars (DA) and argues for a change in the fluvial style represented by a large river.

The preserved fluvial units in the Shafer basin (Goose Neck and Potash) show aggradation of sediments through a tectonically active basin. The aggradation may well have evolved through multiple episodes of interrupting incisions during overall aggradation. Furthermore, the floodplain has been incised and cannibalized by the overlying fluvial units. There are several reasons for fluvial systems to aggrade. First, preservation of the fluvial unit and aggradation is a result of rapid sea-level rise (Skelly et al., 2003). This is not (Loope, 1985) at the time of the FL2 deposition. Secondly, aggradation may have a tectonic origin: decreasing slope owing to subsidence also causes aggradation of fluvial deposits (Posamentier et al., 1992; Schumm, 1993; Wescott, 1993; and Holbrook and Schumm, 1999) as may be the case in the Lower Cutler beds which indicate deposits of the Shafer basin were aggraded through subsidence of the Paradox Foreland Basin. Third, the channel bed aggrades when the sediment supply exceeds the discharge power (Bagnold, 1973). It is conceivable that aggradation records a net increase in sediment supply over the duration of the FL2 unit with interrupted incision events.

4.3 The Canyonland location

The studied fluvial deposit is marked by a river channel belt that has carried some pebble/coarse grains, which are preserved at its base (see Appendix). The studied FL3 unit

outcrop demonstrates a ~ twenty nine meters long fluvial channel belt surface that has nested several low angles channels. The belts are thin and appear to preserve complete to near-complete bars, which implies that the forming channels were shallow.

Fluvial sediments with large and flat bounding surfaces incise into a wet interdune of sand, silt and mud sheets. The wet interdune strata beneath the FL3 unit represents a time when discharge completely drowned aeolian sand bars and re-deposited them as sand laminated sheets. Nonetheless, it may be the raising water-table that created damp surfaces and halted aeolian sand-dune migration.

The Canyonland fluvial unit fines upwards to bar deposits that are completely chaotic and convoluted. This transition marks the top of the fluvial unit which then transitions to limestone recording a trangressive marine incursion (Figure 27). The reduction of sediments is documented by white sandstone at the very top of the fluvial unit in the Canyonland basin. This color transition could be due to an anoxic environment where the sediments were deposited.

The Canyonland fluvial unit geometry and scale of bars and channels deposited up to two to three meters appear to represent deposition within at least three stories of stacked channel belts. Tough cross-bedded point bars seem to have been liquefied throughout the top of the channel belt and did not disturb the whole fluvial outcrop. This is due to local abrupt fault displacement while sediments were saturated beneath the water table. Liquefaction occurs because of the increased pore pressure and reduced effective stress between solid particles generated by the presence of liquid. It is often caused by severe shaking, especially that associated with earthquakes (Dzulynski and Smith, 1963) (Figure 30). The basin in which the FL3 was probably deposited was a lowland coastal river system which would have had a high water table that would have saturated these sands. An earthquake greater than 6.4 Mo could have induced regional liquefaction in these alluvial aquifers much like in the well studied case of the New Madrid seismic zone (Tuttle and Schweig, 1995). This would have mostly affected the upper shallow and less compacted belt and cause regional convolution of these beds. The

source of the earthquake may have been deep and far up to 300 km away from the affected area if the earth quake were large as in the case of the Holocene fault displacement in Tennessee and of the New Madrid seismic zone that liquefied lowland fluvial sands of the Mississippi River floodplain (Tuttle et al., 2006). Synsedimentary regional deformation and liquefaction of sediments during the middle Jurassic due to meteor impact and its seismic effects has also been noticed in the Entrada Formation of southeastern Utah (Alvarez, et al., 1998).

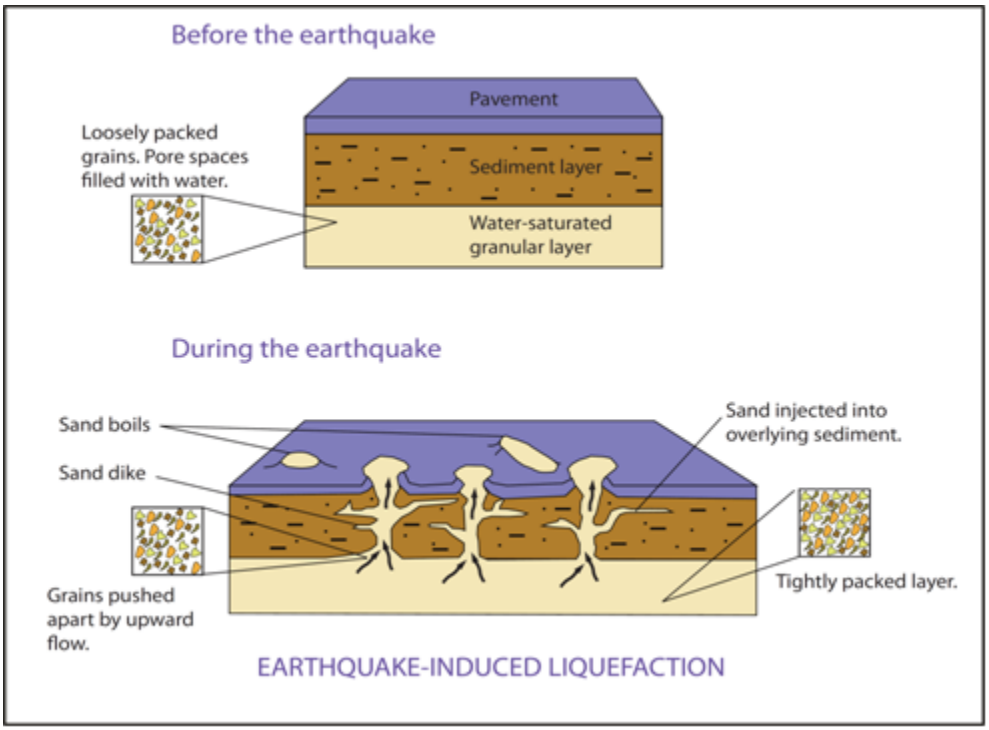

Figure 30: Liquefaction of sediment before and after an earthquake.

Documented channel incisions in the Canyonland basin may indicate deposition within a low accumulation space, yet still high sediment delivery to the proximate shoreline. Fluvial drowning by the overlying marine transgression indicates deposition within a coastal system and transition from fluvial aggradation to landward facies shift as the lowered sea-level buttress began to rise (Zaitlin et al., 1994; Shanley and McCabe, 1994).

In general, the fluvial units of the Canyonland basin are deposited by laterally and vertically amalgamated channel belts. These channel belts bound several channels so that each encompasses mid-channel and lateral accretion point bars. The geometry of the bars is shallow but somewhat wide which could be consistent with a braided fluvial system. Furthermore, similar to the FL2 fluvial section, the Canyonland fluvial unit is also composed of a mix-complex braided meandering system due to the presence of both mid-channel scours and large lateral accretion bars interbedded and incising one another. The top of the belt is marked by the liquefaction of sediment due to seismic activities. The presence of a white sandstone bed that overlies the convoluted beds is suggestive of a deepening water level and invasion of anoxic groundwater and the limestone that tops it is evidence for a large magnitude eustatic sea-level cycle transgression.

The lateral channelizing style could be the result of a decreased buffer zone thickness at the low slopes near the shoreline. The stacking of discrete channel belts without intervening valley incision record steady rise of sea level and deposition near the shore in a buffer zone too thin to support valley reincision as transgression commenced. The Canyonland fluvial unit is inferred to be the distal deposits of fluvial sand migration toward a paleo-shoreline.

CHAPTER 5

CONCLUSIONS

1) Aggradation of Lower Cutler beds is driven by a general subsidence of the basin overprinted by a switch from aeolian to fluvial conditions that generated sequence boundaries below FL2 and Fl3 prior to eventual marine transgression over unit FL3.

2) Fluvial aggradation in the FL2 unit was nonlinear, and was punctuated by episodes of buffer-valley incision that formed higher order surfaces that reflect changes in sediment versus water supply in the discrete drainages or rivers. These valley incision events do not necessarily generate surfaces that correlate beyond the discrete valley. These surfaces produced a partitioned fluvial architecture.

3) Changes in the architecture of the fluvial units across higher order valley surfaces indicate changes in fluvial style associated with renewed aggradation after incision. The architecture of FL2 and FL3 reflects an overall mixture of braided and meandering river systems, rather than a consistent river pattern throughout deposition.

4) The FL2 unit is associated with punctuated aggradation because of its locality remote from the paleo-sea where the buffer zone was thick throughout aggradation and permitted reincision of buffer valleys during the overall aggradational trend. The FL3 units do not record the punctuated aggradation seen in the FL2 unit due to its proximity to the sea and a thin and steadily rising coastal buffer zone.

5) Regional liquefaction at the top of the Canyonland section reflects large (>6.5Mo) earthquakes associated with the end of FL3 deposition.

APPENDIX

ARCHITECTURAL ELEMENT ANALYSIS OF FLUVIAL ROCKS

Architectural Element Analysis of Fluvial Rocks

Shafer basin Location: Strike (left) and dip (right) orientation

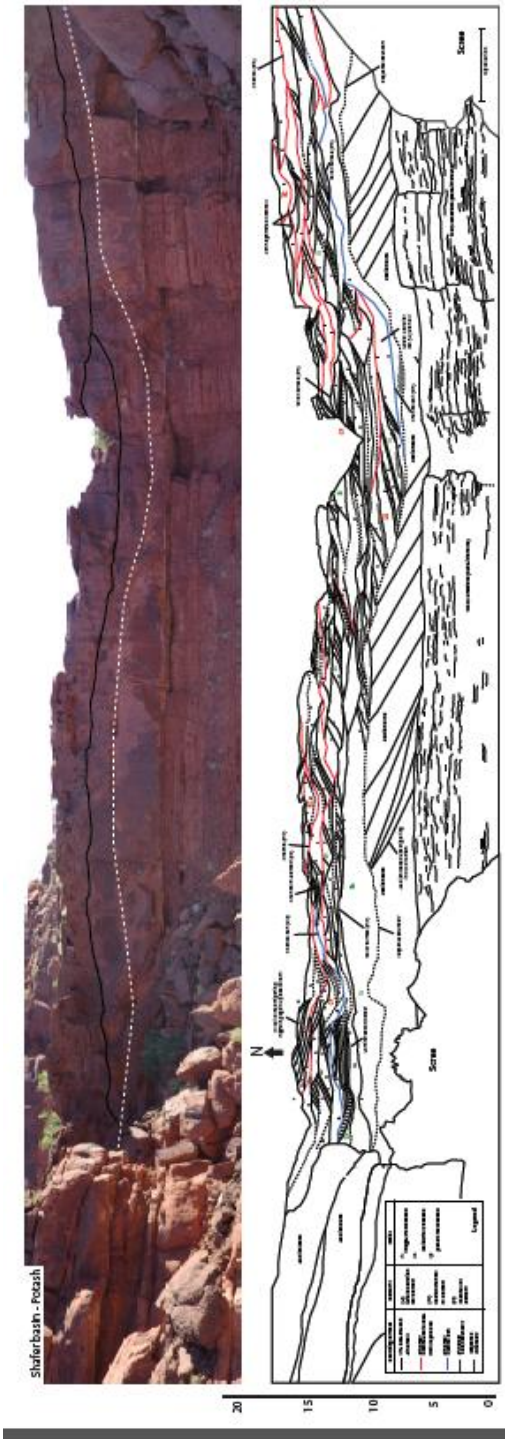

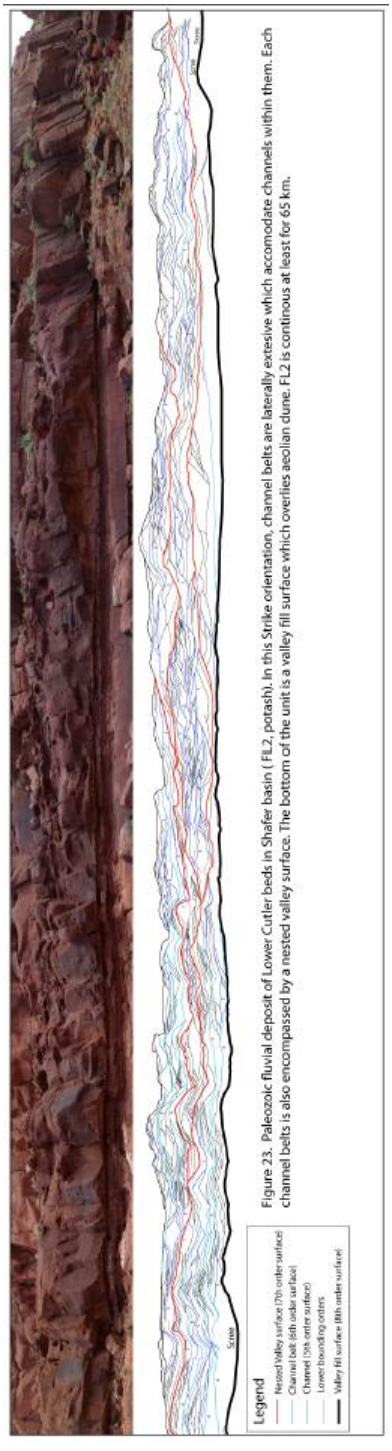

Figure 23. Paleozoic fluvial deposit of Lower Cutler beds in Shafer basin (FL2, potash). In this Strike orientation, channel belts are laterally extesive which accomodate channels within them. Each channel belts is also encompassed by a nested valley surface. The bottom of the unit is a valley fill surface which overlies aeolian dune. FL2 is continous at least for 65 km.

Goose Neck Location

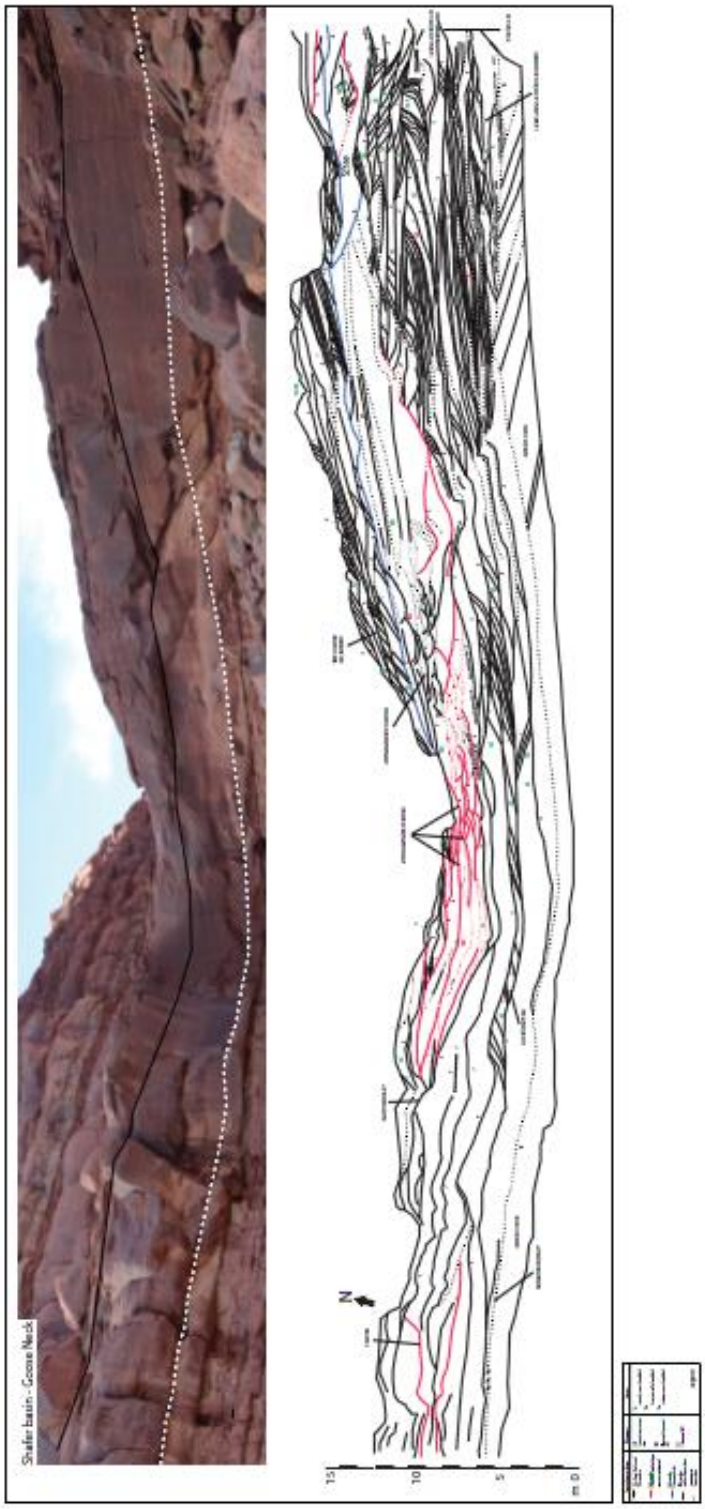

Canyonland basin Location

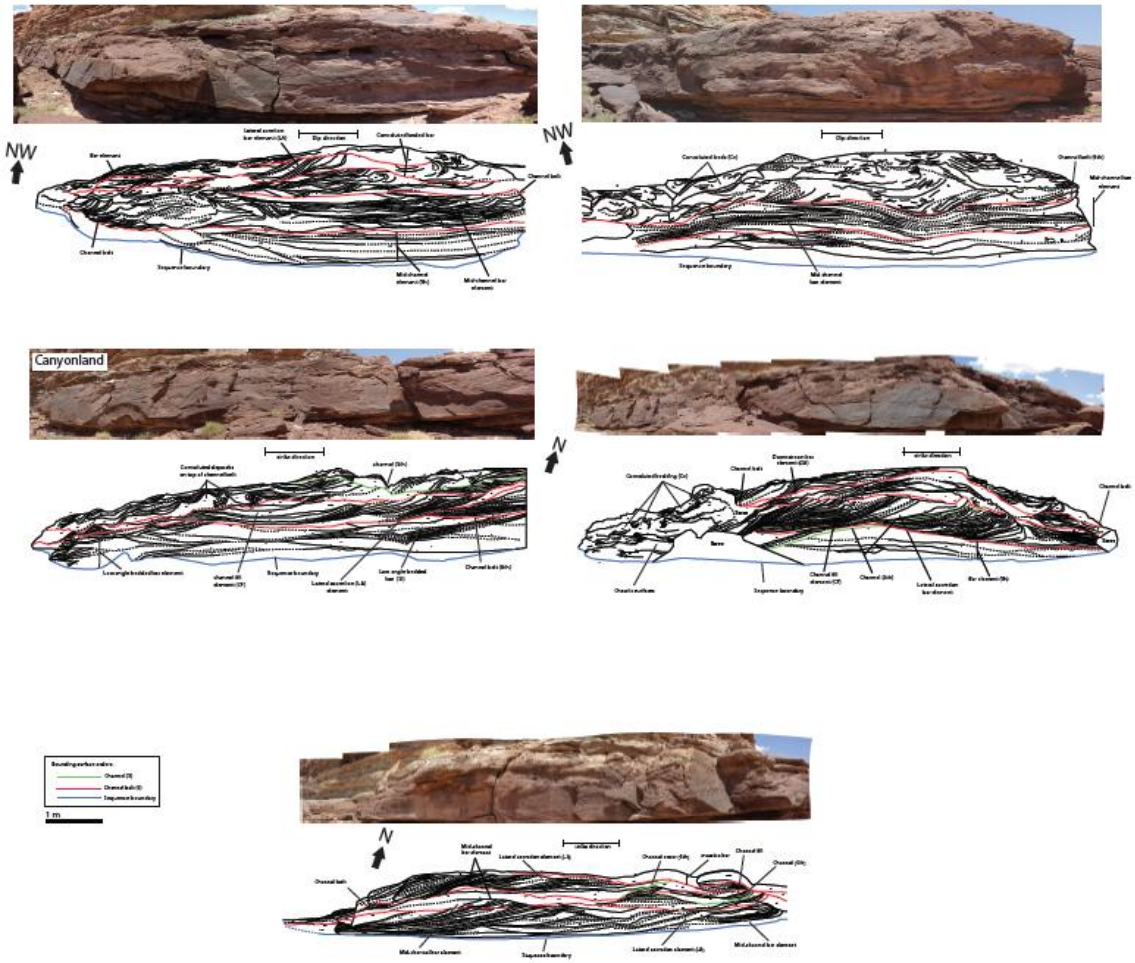

REFERENCES

Allen, J.R.L., 1983, Studies in fluviatile sedimentation; bars, bar-complexes and sandstone sheets (low-sinuosity braided streams) in the Brownstones (L. Devonian), Welsh Borders: Sedimentary Geology, v. 33, p. 237-293.

Allen, J.P., and Fielding, C.R., 2007, Sedimentology and stratigraphic architecture of the Late Permian Betts Creek Beds, Queensland, Australia; Selected papers presented at the Eighth international conference on Fluvial sedimentology: Sedimentary Geology, v. 202, p. 5-34.

Alvarez, W., Staley, E., O'Connor, D., and Chan, M.A., 1998, Synsedimentary deformation in the Jurassic of southeastern Utah; a case of impact shaking? Geology (Boulder), v. 26, p. 579-582.

Bagnold, R.A., 1973, The nature of saltation and of "bed-load" transport in water: Philosophical Transactions of the Royal Society of London, Series A: Mathematical and Physical Sciences, v. 332, p. 473-504.

Barbeau, D.L., 2003, A flexural model for the Paradox Basin; implications for the tectonics of the ancestral Rocky Mountains: Basin Research, v. 15, p. 97-115.

Bridge, J.S., and Diemer, J.A., 1983, Quantitative interpretation of an evolving ancient river system: Sedimentology, v. 30, p. 599-623.

Bromley, R.G., 1996, Trace Fossils: Biology, Taphonomy and Application: Chapman and Hall, pp. 367.

Brookfield, M.E., 1977, The origin of bounding surfaces in ancient aeolian sandstones: Sedimentology, v. 24, p. 303-332.

Brookfield, M.E., 1992, Eolian systems, in Walker, R.G. and James, N.P., eds., Facies models; response to sea level change: Canada (CAN), Geological Association of Canada, St. Johns, NL, Canada (CAN), pp. 143-156.

Cain, S.A., and Mountney, N.P., 2009, Spatial and temporal evolution of a terminal fluvial fan system; the Permian Organ Rock Formation, south-east Utah, USA: Sedimentology, v. 56, p. 1774-1800.

Clarkson, E.N.K., Harper, D.A.T., and Hoeey, A.N., 1998, Basal Wenlock biofacies from the Girvan District, SW Scotland: Scottish Journal of Geology, v. 34, Part 1, p. 61-71.

Collinson, J., 1970, Bedforms of Tana River, Norway: Geografiska Annaler, v. 52, p. 31-51.

Condon, M. S., 1997, Evolution of Sedimentary Basin-Paradox Basin: Geology of the Pennsylvanian-Permian cutler Group and Permian Kaibab Limestone in the Paradox-Basin, Southeastern Utah and Southwestern Colorado: U.S. Geological Survey Bulletin 2000, p. 1-46.

Dzulynski, S., and Smith, A.J., 1963, Convolute lamination, its origin, preservation, and directional significance: Journal of Sedimentary Petrology, v. 33, p. 616-627.

Elias, G.K., 1963, Habitat of Pennsylvanian algal bioherms, Four Corners area; Shelf carbonates of the Paradox basin, a symposium--Four Corners Geol. Soc., 4th Field Conf., p. .

Gibling, M.R., 2006, Width and thickness of fluvial channel bodies and valley fills in the geological record; a literature compilation and classification: Journal of Sedimentary Research, v. 76, p. 731-770.

Halley, R.B., and Schmoker, J.W., 1983, High-porosity Cenozoic carbonate rocks of South Florida; progressive loss of porosity with depth: AAPG Bulletin, v. 67, p. 191-200.

Haszeldine, R.S., 1983, Fluvial bars reconstructed from a deep, straight channel, Upper Carboniferous coalfield of Northeast England: Journal of Sedimentary Petrology, v. 53, p. 1233-1247.

Holbrook, J., and Schumm, S.A., 1999, Geomorphic and sedimentary response of rivers to tectonic deformation; a brief review and critique of a tool for recognizing subtle

epeirogenic deformation in modern and ancient settings; Tectonics of continental interiors: Tectonophysics, v. 305, p. 287-306.

Holbrook, J., 2001, Origin, genetic interrelationships, and stratigraphy over the continuum of fluvial channel-form bounding surfaces; an illustration from Middle Cretaceous strata, southeastern Colorado: Sedimentary Geology, v. 144, p. 179-222.

Holbrook, J., Scott, R.W., and Oboh-Ikuenobe, F.E., 2006, Base-level buffers and buttresses; a model for upstream versus downstream control on fluvial geometry and architecture within sequences: Journal of Sedimentary Research, v. 76, p. 162-174.

Hunter, R.E., 1977, Terminology of cross-stratified sedimentary layers and climbing-ripple structures: Journal of Sedimentary Petrology, v. 47, p. 697-706.

Jordan, O.D., and Mountney, N.P., 2010, Styles of interaction between aeolian, fluvial and shallow marine environments in the Pennsylvanian to Permian lower Cutler beds, south-east Utah, USA: Sedimentology, v. 57, p. 1357-1385.

Kelley, V.C., 1958, Tectonics of the region of the Paradox Basin - Guidebook to the geology of the Paradox Basin. p. 31-38.

Langford, R.P., and Chan, M.A., 1989, Fluvial-aeolian interactions; Part II, Ancient systems: Sedimentology, v. 36, p. 1037-1051.

Leopold, L., and Wolfman, G., 1957, River Channel Patterns: Braided, Meandering, and Straight: Geological Survey Professional Paper 282- B, p. 39-89.

Loope, D.B., 1985, Episodic deposition and preservation of eolian sands; a late Paleozoic example from southeastern Utah: Geology (Boulder), v. 13, p. 73-76.

Loope, D.B., 1984, Eolian origin of upper Paleozoic sandstones, southeastern Utah: Journal of Sedimentary Petrology, v. 54, p. 563-580.

Mack, G.H., 1977, Depositional environments of the Cutler-Cedar Mesa facies transition (Permian) near Moab, Utah: The Mountain Geologist, v. 14, p. 53-68.

Mack, G.H., 1978, The survivability of labile light-mineral grains in fluvial, aeolian and littoral marine environments; the Permian Cutler and Cedar Mesa formations, Moab, Utah: Sedimentology, v. 25, p. 587-603.

McKee, E.D., and Weir, G.W., 1953, Terminology for stratification and crosstratification in sedimentary rocks: Geological Society of America Bulletin, v. 64, p. 381-389.

McKnight, E.T., 1958, Geology of area between Green and Colorado rivers, Grand and San Juan counties, Utah: Geological Survey Bulletin 908, p. 147.

Miall, A.D., 1985, Architectural-element analysis; a new method of facies analysis applied to fluvial deposits: Earth-Science Reviews, v. 22, p. 261-308.

Miall, A.D., 1988a, Architectural elements and bounding surfaces in fluvial deposits; anatomy of the Kayenta Formation (Lower Jurassic), Southwest Colorado: Sedimentary Geology, v. 55, p. 233-262.

Miall, A. D., 1988b, Facies architecture in clastic sedimentary basins, in Kleinspehn, K., and Paola, C., eds., New perspectives in basin analysis: New York, Springer-Verlag, p. 63–81.

Miall, A.D., 1991, Stratigraphic sequences and their chronostratigraphic correlation: Journal of Sedimentary Petrology, v. 61, p. 497-505.

Miall, A.D., and Tyler, N., 1991, Hierarchies of architectural units in terrigenous clastic rocks, and their relationship to sedimentation rate; The three-dimensional facies architecture of terrigenous clastic sediments and its implications for hydrocarbon discovery and recovery: Concepts in Sedimentology and Paleontology, v. 3, p. 6-12.

Miall, A.D., 1992, Exxon global cycle chart; an event for every occasion? Geology (Boulder), v. 20, p. 787-790.

Miall, A.D., 1996, The geology of fluvial deposits; sedimentary facies, basin analysis, and petroleum geology: Federal Republic of Germany (DEU), Springer-Verlag, Berlin, Federal Republic of Germany (DEU), p. 582.

Peterson, J.A., and Hite, R.J., 1969, Pennsylvanian evaporite-carbonate cycles and their relation to petroleum occurrence, southern Rocky Mountains; Evaporites and petroleum: The American Association of Petroleum Geologists Bulletin, v. 53, p. 884-908.

Posamentier, H.W., Allen, G.P., James, D.P., and Tesson, M., 1992, Forced Regression in a Stratigraphic Framework: Concepts, Examples, and Exploration Significance: AAPG Bulletin, v. 76, p. 1687-1701.

Pray, L.C., and Wray, J.L., 1963, Porous algal facies (Pennsylvanian), Honaker Trail, San Juan Canyon, Utah: Four Corners Geological Society Symposium, Shelf Carbonates of the Paradox Basin. Four Corners Geological Society, 4th Field Conference: p. 204-234.

Rodriguez, A.B., Anderson, J.B., and Simms, A.R., 2005, Terrace inundation as an autocyclic mechanism for parasequence formation; Galveston Estuary, Texas, U.S.A: Journal of Sedimentary Research, v. 75, p. 608-620.

Schumm, S., 1968, River Adjustment to Altered Hydrologic Regimen-Murrumbidgee River and Paleochannels, Australia: Geological Survey Professional Paper 598, p. 1-65.

Schumm, S.A., 1993, River response to baselevel change; implications for sequence stratigraphy; Centennial special issue: Journal of Geology, v. 101, p. 279-294.

Shanley, K.W., and McCabe, P.J., 1994, Perspectives on the sequence stratigraphy of continental strata: AAPG Bulletin, v. 78, p. 544-568.

Skelly, R.L., Bristow, C.S., and Ethridge, F.G., 2003, Architecture of channel-belt deposits in an aggrading shallow sandbed braided river; the lower Niobrara River, Northeast Nebraska: Sedimentary Geology, v. 158, p. 249-270.

Strong, N., and Paola, C., 2008, Valleys that never were; time surfaces versus stratigraphic surfaces: Journal of Sedimentary Research, v. 78, p. 579-593.

Terrell, F.M., 1972, Lateral Facies and Paleoecology of Permian Elephant Canyon Formation, Grand County, Utah: Brigham Young University Research Studies, Geology Series, v. 19, p. 3-44.

Tucker, M.E., Wright, V.P., and Dickson, J.A.D., 1990, Carbonate sedimentology: United Kingdom (GBR), Blackwell Sci. Publ., Oxford, United Kingdom (GBR), p. .

Tuttle, M.P., Al-Shukri, H., and Mahdi, H., 2006, Very large earthquakes centered southwest of the New Madrid seismic zone 5,000-7,000 years ago: Seismological Research Letters, v. 77, p. 755-770.

Tuttle, M.P., and Schweig, E.S., 1995, Archeological and pedological evidence for large prehistoric earthquakes in the New Madrid seismic zone, central United States: Geology (Boulder), v. 23, p. 253-256.

Wengerd, S.A., and Matheny, M.L., 1958, Pennsylvanian system of Four Corners Region: Bulletin of the American Association of Petroleum Geologists, v. 42, p. 2048-2106.

Wescott, W.A., 1993, Geomorphic thresholds and complex response of fluvial systems; some implications for sequence stratigraphy: AAPG Bulletin, v. 77, p. 1208-1218.

Zaitlin, B.A., Dalrymple, R.W., and Boyd, R., 1994, The stratigraphic organization of incised-valley systems associated with relative sea-level change: SEPM, p. 45-62.

BIOGRAPHICAL INFORMATION

Siavash Rastaghi was born in Shiraz, Iran on June 22nd of 1976. He immigrated to the U.S. with his family in 1998. He received his B.A. in Biology from the University of Texas at Dallas in 2005. He started his M.S. in Geology at UT Dallas in the fall of 2006; however, he transferred to the University of Texas at Arlington in 2008 where he received his M.S. in Geology (Sedimentology) under the supervision and mentorship of John M. Holbrook. He currently lives in North Dallas, Texas and will pursue his PhD in Geology.